An Adaptive Quantum Circuit of Dempster's Rule of Combination for Uncertain Pattern Classification

Fuyuan Xiao*
School of Big Data and Software Engineering
Chongqing University
Chongqing, China 401331
xiaofuyuan@cqu.edu.cn

Yu Zhou
School of Big Data and Software Engineering
Chongqing University
Chongqing, China 401331

Witold Pedrycz
Department of Electrical and Computer Engineering
University of Alberta
Edmonton, AB T6G 2R3, Canada
Systems Research Institute, Polish Academy of Sciences
00-901 Warsaw, Poland,
National Information Processing Institute
00-608 Warsaw, Poland
wpedrycz@ualberta.ca

Abstract

In pattern classification, efficient uncertainty reasoning plays a critical role, particularly in real-time applications involving noisy data, ambiguous class boundaries, or overlapping categories. Leveraging the advanced computational power of quantum computing, an Adaptive Quantum Circuit for Dempster's Rule of Combination (AQC-DRC) is proposed to address efficient classification under uncertain environments. The AQC-DRC is developed within the framework of quantum evidence theory (QET) and facilitates decision-making based on quantum basic probability and plausibility levels, which is a generalized Bayesian inference method. The AQC-DRC provides a deterministic computation of DRC, ensuring that quantum fusion outcomes in uncertain pattern classification are exactly aligned with those of the classical method, while simultaneously achieving exponential reductions in the computational complexity of evidence combination and significantly improving fusion efficiency. It is founded that the quantum basic probability amplitude function in QET, as a generalized quantum probability amplitude, can be naturally utilized to express the quantum amplitude encoding. In addition, the quantum basic probability in QET, as a generalized quantum probability, naturally forms a quantum basic probability distribution and can be used to represent quantum measurement outcomes for quantum basic probability level decision-making. Furthermore, the quantum plausibility function in QET also can be naturally used to express the quantum measurement outcomes for quantum plausibility level decision-making. These findings enrich the physical understanding of quantum amplitude encoding and quantum measurement outcomes, offering broad application prospects for representing and processing uncertain knowledge in pattern classification.

*Corresponding author: Fuyuan Xiao

39th Conference on Neural Information Processing Systems (NeurIPS 2025).

1 Introduction

Uncertainty and its dynamics is inherent in many real-world scenarios such as medical diagnosis, intelligent transportation, financial risk assessment, fault detection, and multi-sensor data fusion [1–6]. In the field of pattern classification, uncertainty reasoning is also essential, particularly when data are noisy, class boundaries are ambiguous, or there is overlap between categories. Properly modeling uncertainty in these situations contributes to enhanced robustness and reliability of classification systems [7–10]. To address uncertainty reasoning in such complex environments, numerous theories and methods have been proposed, including Dempster-Shafer evidence theory [11, 12], evidential reasoning [13, 14], D number theory [15], belief rule base [16], complex evidence theory [17], random permutation sets [18–22], and quantum evidence theory [23, 24], among others [25]. These approaches provide solid theoretical foundations and practical tools for modeling and managing uncertainty in various areas, such as evolutionary games [26, 27], network intrusion detection [28], classification [29, 30], social dilemma experiments [31–33], and reliability evaluation [34].

As an effective approach for uncertainty reasoning, DempsterShafer evidence theory (DSET) [11, 12] offers a powerful framework for representing and managing uncertainty through the basic probability assignment (BPA) function [35–37]. The Dempster's rule of combination (DRC) [11], a core component of DSET, possesses several desirable properties that make it particularly suitable for multisource information fusion [38–41], image segmentation [42]. time series [43], decision making [44, 45], engineering management [46], and others [47]. (1) Commutativity: ensures that the fusion result remains invariant regardless of the order in which evidence is combined; (2) Associativity: provides the system with flexible capabilities for structured and sequential fusion; and (3) Consistency: guarantees that, in the absence of new valid information, the outcome of the evidence combination remains unchanged. These advantages support flexible integration of multisource information, enable recursive and incremental computation, and facilitate the scalability of reasoning systems [48]. However, the computational complexity of DRC increases exponentially with the number of elements in the frame of discernment [49, 50].

The rapid development of quantum computing offers a new research perspective for addressing the computational complexity challenges in Dempster's rule of combination of DempsterShafer evidence theory [51–56]. Leveraging the principles of quantum parallelism and quantum entanglement, quantum computing provides the potential to significantly accelerate the processing of large-scale uncertain information with extensive applications [57–61]. In particular, it opens up new possibilities for overcoming the exponential computation complexity issues inherent in classical evidence reasoning frameworks based on DRC, thus providing an innovative approach to efficient information fusion and decision-making [62].

Leveraging the advanced computational power of quantum computing, an Adaptive Quantum Circuit for Dempster's Rule of Combination (AQC-DRC) is proposed to address efficient classification under uncertain environments. The AQC-DRC is developed within the framework of quantum evidence theory (QET) and facilitates decision-making based on quantum basic probability and plausibility levels, which is a generalized quantum Bayesian inference method. The AQC-DRC provides a deterministic computation of DRC, ensuring that quantum fusion outcomes in uncertain pattern classification are exactly aligned with those of the classical method, while simultaneously achieving exponential reductions in the computational complexity of evidence combination and significantly improving fusion efficiency.

In this study, it is founded that the quantum basic probability amplitude (QBPA) function in QET [23, 24], as a generalized quantum probability amplitude, can be naturally used to express the quantum amplitude encoding. In addition, the quantum basic probability (QBP) in QET, as a generalized quantum probability, naturally forms a quantum basic probability distribution (QBPD) and can be used to represent quantum measurement outcomes for basic probability level decision-making. Furthermore, the quantum plausibility (QPl) function in QET also can be naturally used to express the quantum measurement outcomes for quantum plausibility level decision-making. These findings open new perspectives and enrich the physical understanding of quantum amplitude encoding and quantum measurement outcomes, offering broad application prospects for representing and processing uncertain knowledge in areas such as pattern classification, recognition, and decision-making.

2 Preliminaries

2.1 DSET: DempsterShafer evidence theory [11, 12]

Definition 1 (Frame of discernment)**.** *Let Ω be a frame of discernment (FOD), consisting of a set of mutually exclusive and collectively nonempty events:*

$$\Omega = \{h_1, h_2, \ldots, h_i, \ldots, h_n\}. \tag{1}$$

Let 2^Ω be the power set of Ω, denoted as:

$$2^\Omega = \{\emptyset, \{h_1\}, \{h_2\}, \ldots, \{h_n\}, \{h_1, h_2\}, \ldots, \{h_1, h_2, \ldots, h_i\}, \ldots, \Omega\}, \tag{2}$$

where $\emptyset$ is an empty set [63–65].

Definition 2 (Hypothesis or proposition)**.** *H_j is defined as a hypothesis or proposition when $H_j \subseteq \Omega$.*

Definition 3 (Basic probability assignment)**.** *In FOD Ω, a basic probability assignment (BPA) or basic belief assignment (BBA) m, also called a mass function, is defined as a mapping:*

$$m: \quad 2^\Omega \to [0, 1], \tag{3}$$

satisfying

$$m(\emptyset) = 0 \quad \textit{and} \sum_{H_j \subseteq \Omega} m(H_j) = 1. \tag{4}$$

Definition 4 (Focal element)**.** *Let m be a BPA. $\forall H_j \subseteq \Omega$, if $m(H_j) > 0$, H_j is called a focal element in DSET.*

Definition 5 (Plausibility function)**.** *Let H_j and H_t be two propositions such that $H_j, H_t \subseteq \Omega$. A plausibility function Pl, mapping from 2^Ω to $[0, 1]$, is defined by*

$$Pl(H_j) = \sum_{H_t \cap H_j \neq \emptyset} m(H_t) = 1 - Bel(\bar{H}_j), \quad \bar{H}_j = \Omega - H_j, \tag{5}$$

in which the belief function $Bel(\bar{H}_j) = \sum_{H_t \subseteq \bar{H}_j} m(H_t)$, measuring the strength of the evidence in favor of a proposition $\bar{H}_j$.

Definition 6 (Dempster's rule of combination)**.** *Let m_1 and m_2 be two independent BPAs in FOD Ω with propositions $H_t, H_h \subseteq \Omega$, respectively. Dempster's rule of combination (DRC), represented in the form $m_1 \oplus m_2$, is defined by*

$$m_1 \oplus m_2(H_j) = \begin{cases} \dfrac{1}{1-K} \displaystyle\sum_{H_t \cap H_h = H_j} m_1(H_t) m_2(H_h), & H_j \neq \emptyset, \\ 0, & H_j = \emptyset, \end{cases} \tag{6}$$

with the conflict coefficient K between m_1 and m_2:

$$K = \sum_{H_t \cap H_h = \emptyset} m_1(H_t) m_2(H_h). \tag{7}$$

2.2 QET: Quantum evidence theory [23, 24]

Definition 7 (Quantum frame of discernment)**.** *Let Φ be a quantum frame of discernment (QFOD), consisting of a set of mutually exclusive and collectively nonempty events, each of which is expressed as an orthonormal basis ϕ_g in a Hilbert space:*

$$\Phi = \{\phi_1, \ldots, \phi_g, \ldots, \phi_n\}. \tag{8}$$

Let 2^Φ be the power set of Φ, denoted as:

$$2^\Phi = \{\emptyset, \{\phi_1\}, \{\phi_2\}, \ldots, \{\phi_n\}, \{\phi_1\phi_2\}, \ldots, \{\phi_1\phi_2 \ldots \phi_g\}, \ldots, \Phi\}, \tag{9}$$

which can be simply represented as ($\emptyset$ is an empty set):

$$2^\Phi = \{\emptyset, \phi_1, \phi_2, \ldots, \phi_n, \phi_{12}, \ldots, \phi_{12\ldots g}, \ldots, \phi_{12\ldots n}\}. \tag{10}$$

Definition 8 (Quantum hypothesis or proposition)**.** *ψ_j is defined as a quantum hypothesis or proposition when $\psi_j \subseteq \Phi$.*

Definition 9 (Quantum basic probability amplitude function)**.** *A quantum basic probability amplitude (QBPA) function $\mathbb{Q}_{\mathbb{M}}$ in QFOD Φ, also referred to as a quantum mass function, is defined as a mapping:*

$$\mathbb{Q}_{\mathbb{M}} : 2^{\Phi} \to \mathbb{C}, \tag{11}$$

satisfying

$$\begin{aligned} \mathbb{Q}_{\mathbb{M}}(\emptyset) = 0 \quad \textit{and} \quad \mathbb{Q}_{\mathbb{M}}(\psi_j) = \varphi(\psi_j) e^{i\theta(\psi_j)}, \quad \psi_j \subseteq \Phi, \\ \sum_{\psi_j \subseteq \Phi} |\mathbb{Q}_{\mathbb{M}}(\psi_j)|^2 = 1, \end{aligned} \tag{12}$$

in which $i = \sqrt{-1}$; $\varphi(\psi_j) \in [0, 1]$ represents the modulus of $\mathbb{Q}_{\mathbb{M}}(\psi_j)$; $\theta(\psi_j)$ denotes a phase term of $\mathbb{Q}_{\mathbb{M}}(\psi_j)$; and $|\mathbb{Q}_{\mathbb{M}}(\psi_j)|^2 = \varphi^2(\psi_j)$ denotes the modulus squared of $\mathbb{Q}_{\mathbb{M}}(\psi_j)$.

Note that, QBPA is a generalized quantum probability amplitude. When the QBPA are only assigned to singleton states, the QBPA is referred to as quantum probability amplitude.

Definition 10 (Quantum focal element)**.** *Let $\mathbb{Q}_{\mathbb{M}}$ be a QBPA. $\forall \psi_j \subseteq \Phi$, if $|\mathbb{Q}_{\mathbb{M}}(\psi_j)|$ or $\varphi(\psi_j) > 0$, ψ_j is called a quantum focal element in QET.*

Definition 11 (Quantum basic probability function)**.** *The quantum basic probability function of $\mathbb{Q}_{\mathbb{M}}$, also referred as a quantum basic probability distribution (QBPD), is defined as:*

$$\mathrm{M} : 2^{\Phi} \to [0, 1], \tag{13}$$

and satisfies:

$$\begin{aligned} \mathrm{M}(\emptyset) = 0 \quad \textit{and} \quad \mathrm{M}(\psi_j) = |\mathbb{Q}_{\mathbb{M}}(\psi_j)|^2, \quad \psi_j \subseteq \Phi, \\ \sum_{\psi_j \subseteq \Phi} \mathrm{M}(\psi_j) = 1, \end{aligned} \tag{14}$$

where $|\mathbb{Q}_{\mathbb{M}}(\psi_j)|^2 = \mathbb{Q}_{\mathbb{M}}(\psi_j)\widehat{\mathbb{Q}}_{\mathbb{M}}(\psi_j) = \varphi^2(\psi_j) = x_j^2 + y_j^2$, in which $\widehat{\mathbb{Q}}_{\mathbb{M}}(\psi_j)$ is the complex conjugate of $\mathbb{Q}_{\mathbb{M}}(\psi_j)$, e.g., $\widehat{\mathbb{Q}}_{\mathbb{M}}(\psi_j) = x_j - y_j i$; and $\mathrm{M}(\psi_j)$ $(\psi_j \subseteq \Phi)$ is called quantum basic probability (QBP), which represents the observed degree of belief or support to ψ_j.

Note that, QBP is a generalized quantum probability. When the quantum basic probability are only assigned to singleton states, the QBP is referred to as quantum probability.

Definition 12 (Quantum plausibility function)**.** *Let $\mathbb{Q}_{\mathbb{M}}$ be a QBPA with proposition $\psi_j \subseteq \Phi$. A quantum plausibility (QPl) function in QET, mapping from 2^{Φ} to $[0, 1]$, is defined by:*

$$\mathit{QPl}(\psi_j) = \sum_{\psi_p \cap \psi_j \neq \emptyset} \left| \mathbb{Q}_{\mathbb{M}}(\psi_p) \right|^2, \quad \psi_j \subseteq \Phi. \tag{15}$$

According to Eq. (14), Eq. (15) can also be represented as:

$$\mathrm{QPl}(\psi_j) = \sum_{\psi_p \cap \psi_j \neq \emptyset} \varphi^2(\psi_j) = \sum_{\psi_p \cap \psi_j \neq \emptyset} \mathrm{M}(\psi_p), \quad \psi_j \subseteq \Phi. \tag{16}$$

Therefore, when $\mathrm{M} = m$, Eq. (16) becomes:

$$\mathrm{QPl}(\psi_j) = \sum_{\psi_p \cap \psi_j \neq \emptyset} m(\psi_p), \quad \psi_j \subseteq \Phi, \tag{17}$$

which is consistent with the classical Pl in DSET.

3 AQC-DRC: Adaptive Quantum Circuit for Dempster's Rule of Combination

The AQC-DRC consists of the following three components: 1) quantum amplitude encoding for BPA, 2) construction of the adaptive quantum circuit for DRC, and 3) measurement in the adaptive quantum circuit for decision-making. The flowchart is displayed in Fig. 1.

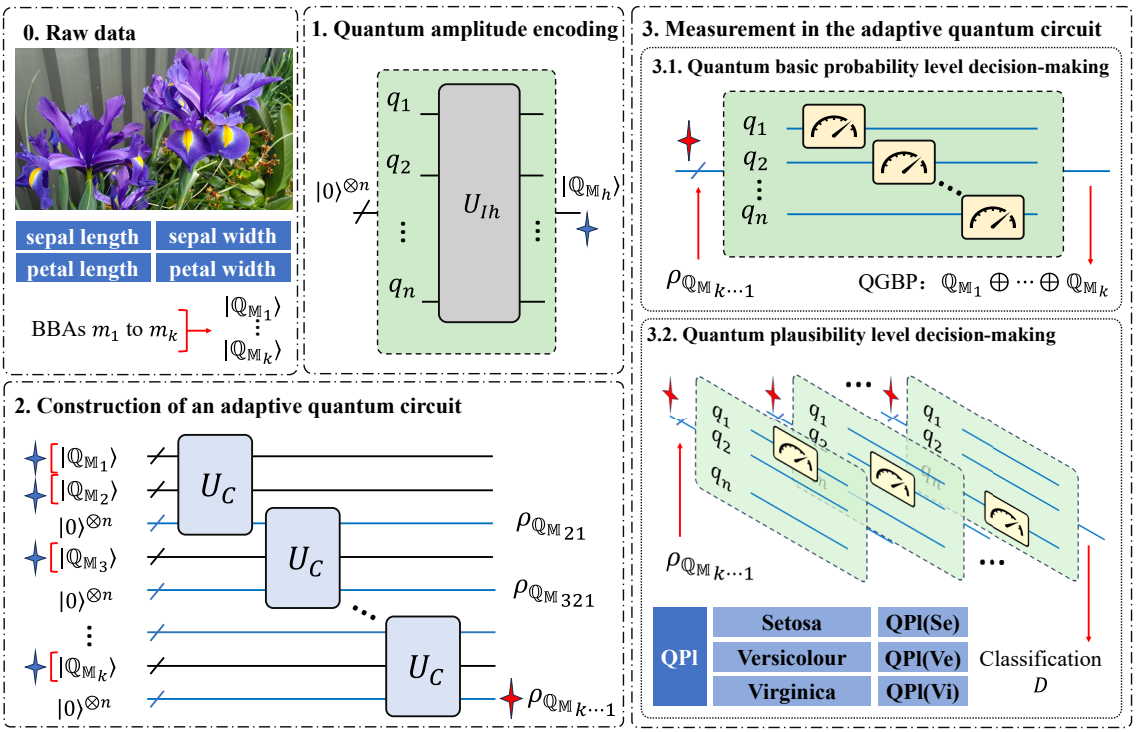

Figure 1: The flowchart of the adaptive quantum circuit for Dempster's rule of combination.

3.1 Quantum amplitude encoding for BPA

In this section, the QBPA in QET is expressed for quantum amplitude encoding mechanism. In this context, a BPA is encoded as a superposition over an n-qubit quantum state.

Definition 13 (QBPA-based quantum amplitude encoding mechanism)**.** *Let $\mathbb{Q}_{\mathbb{M}}$ be a QBPA on the QFOD $\Phi = \{\phi_1, \ldots, \phi_i, \ldots, \phi_n\}$ with quantum proposition $\psi_j \subseteq \Phi$. The QBPA-based quantum amplitude encoding mechanism, also referred to as the quantum superposition state of the QBPA, is defined as:*

$$\begin{aligned} |\mathbb{Q}_{\mathbb{M}}\rangle &= \sum_{\psi_j \subseteq \Phi} \mathbb{Q}_{\mathbb{M}}(\psi_j)|\psi_j\rangle = \sum_{\psi_j \subseteq \Phi} \varphi(\psi_j) e^{i\theta(\psi_j)}|\psi_j\rangle, \\ \sum_{\psi_j \subseteq \Phi} |\mathbb{Q}_{\mathbb{M}}(\psi_j)|^2 &= \sum_{\psi_j \subseteq \Phi} \varphi^2(\psi_j) = 1, \end{aligned} \tag{18}$$

where

$$|\psi_j\rangle = \bigotimes_{i=1}^{n} |\delta_{ji}\rangle = |\delta_{jn}\rangle \cdots |\delta_{ji}\rangle \cdots |\delta_{j2}\rangle|\delta_{j1}\rangle = |\delta_{jn} \cdots \delta_{ji} \cdots \delta_{j2}\delta_{j1}\rangle, \tag{19}$$

and

$$\delta_{ji} = \begin{cases} 1, & \text{if } \phi_i \in \psi_j, \\ 0, & \text{if } \phi_i \notin \psi_j. \end{cases} \tag{20}$$

When $\theta(\psi_j) = 0$, the QBPA expression for quantum amplitude encoding can be represented as:

$$|\mathbb{Q}_{\mathbb{M}}\rangle = \sum_{\psi_j \subseteq \Phi} \varphi(\psi_j)|\psi_j\rangle, \quad \text{and} \quad \sum_{\psi_j \subseteq \Phi} \varphi^2(\psi_j) = 1. \tag{21}$$

Definition 14 (Quantum amplitude encoding of BPA)**.** *Let m_h be a BPA on the FOD $\Phi = \{\phi_1, \ldots, \phi_i, \ldots, \phi_n\}$ with proposition $\psi_j \subseteq \Phi$. Considering QBPA-based quantum amplitude encoding mechanism, a BPA m_h is encoded into the amplitudes of an n-qubit state as:*

$$|\mathbb{Q}_{\mathbb{M}_h}\rangle = U_E(m_h)|0\rangle^{\otimes n} = \sum_{\psi_j \subseteq \Phi} \mathbb{Q}_{\mathbb{M}_h}(\psi_j)|\psi_j\rangle = \sum_{\psi_j \subseteq \Phi} \varphi_h(\psi_j) e^{i\theta_h(\psi_j)}|\psi_j\rangle, \tag{22}$$

satisfying

$$\varphi_h(\psi_j)e^{i\theta_h(\psi_j)} = \sqrt{m_h(\psi_j)}e^{i0} = \sqrt{m_h(\psi_j)}, \quad \textit{and} \quad \sum_{\psi_j \subseteq \Phi} \left|\sqrt{m_h(\psi_j)}\right|^2 = 1, \tag{23}$$

where $|\psi_j\rangle$ is defined in Definition 13, and U_E denotes a state preparation oracle or operator.

Each BPA m_h is encoded as a superposition over an n-qubit quantum state with regards to the QBPA-based quantum amplitude encoding mechanism. Therefore, a collection of k BPAs $\{m_1, \ldots, m_h, \ldots, m_k\}$ is encoded to a set of k distinct n-qubit quantum states $\{|\mathbb{Q}_{\mathbb{M}_1}\rangle, \ldots, |\mathbb{Q}_{\mathbb{M}_h}\rangle, \ldots, |\mathbb{Q}_{\mathbb{M}_k}\rangle\}$ with $|\mathbb{Q}_{\mathbb{M}_h}\rangle = U_E(m_h)|0\rangle^{\otimes n}$.

3.2 Construction of an adaptive quantum circuit for DRC

The encoded quantum states $\{|\mathbb{Q}_{\mathbb{M}_1}\rangle, \ldots, |\mathbb{Q}_{\mathbb{M}_h}\rangle, \ldots, |\mathbb{Q}_{\mathbb{M}_k}\rangle\}$ corresponding to the k BPAs $\{m_1, \ldots, m_h, \ldots, m_k\}$ will be combined by a series of specific quantum operators, which is categorized as one types of U_C designed through Toffoli gates.

To be specific, two encoded quantum states $|\mathbb{Q}_{\mathbb{M}_1}\rangle$ and $|\mathbb{Q}_{\mathbb{M}_2}\rangle$ are considered corresponding to the BPAs m_1 and m_2, the inputs of U_C are $|\mathbb{Q}_{\mathbb{M}_1}\rangle$, $|\mathbb{Q}_{\mathbb{M}_2}\rangle$, and $|0\rangle^{\otimes n}$-qubit. After applying U_C based on the Toffoli gate, the output is mapped to $|0\rangle^{\otimes n}$ qubits, which serve as auxiliary qubits for storing the processed information. Subsequently, a partial trace over the subsystem $\{\mathbb{Q}_{\mathbb{M}_2}, \mathbb{Q}_{\mathbb{M}_1}\}$ is performed using $\mathrm{Tr}_{(\mathbb{Q}_{\mathbb{M}_2}\mathbb{Q}_{\mathbb{M}_1})}$ to obtain the reduced density matrix $\rho_{\mathbb{Q}_{\mathbb{M}_{21}}}$, which characterizes the state of the subsystem $\rho_{\mathbb{Q}_{\mathbb{M}_{21}}}$:

$$\begin{aligned}
\rho_{\mathbb{Q}_{\mathbb{M}_{21}}} &= \mathrm{Tr}_{(\mathbb{Q}_{\mathbb{M}_2}\mathbb{Q}_{\mathbb{M}_1})}\left(U_C|0\rangle^{\otimes n}\langle 0|^{\otimes n} \otimes |\mathbb{Q}_{\mathbb{M}_2}\rangle\langle\mathbb{Q}_{\mathbb{M}_2}| \otimes |\mathbb{Q}_{\mathbb{M}_1}\rangle\langle\mathbb{Q}_{\mathbb{M}_1}|U_C^\dagger\right) \\
&= \mathrm{Tr}_{(\mathbb{Q}_{\mathbb{M}_2}\mathbb{Q}_{\mathbb{M}_1})}\left(U_C|0\rangle^{\otimes n}\langle 0|^{\otimes n} \otimes \rho_{\mathbb{Q}_{\mathbb{M}_2}} \otimes \rho_{\mathbb{Q}_{\mathbb{M}_1}}U_C^\dagger\right) \\
&= \sum_{\psi_t \subseteq \Phi} \sum_{\cap\psi_j = \psi_t} \prod_{1 \le h \le 2} \left|\varphi_h(\psi_j)e^{i\theta_h(\psi_j)}\right|^2 |\psi_t\rangle\langle\psi_t| \\
&= \sum_{\psi_t \subseteq \Phi} \sum_{\cap\psi_j = \psi_t} \prod_{1 \le h \le 2} \left|\sqrt{m_h(\psi_j)}\right|^2 |\psi_t\rangle\langle\psi_t|,
\end{aligned} \tag{24}$$

where $|\psi_t\rangle$ is defined in Definition 13. It is concluded that for arbitrary two encoded quantum states corresponding to the BPAs, a U_C operator of the Toffoli gate is implemented.

Hence, h $(2 \le h \le k)$ encoded quantum states $\{|\mathbb{Q}_{\mathbb{M}_1}\rangle, \ldots, |\mathbb{Q}_{\mathbb{M}_h}\rangle\}$ are considered corresponding to the BPAs $\{m_1, \ldots, m_h\}$, $h-1$ U_C operations based on Toffoli gates are recursively implemented in accordance with the DRC to fuse h BPAs. Following the recursive application of the $(h-1)$-th U_C Toffoli gate, we perform a partial trace over the subsystem $\{\mathbb{Q}_{\mathbb{M}_h}, \ldots, \mathbb{Q}_{\mathbb{M}_1}\}$ using $\mathrm{Tr}_{(\mathbb{Q}_{\mathbb{M}_h}\ldots\mathbb{Q}_{\mathbb{M}_1})}$ to obtain the reduced density matrix $\rho_{\mathbb{Q}_{\mathbb{M}_{h\ldots1}}}$, which characterizes the state of the corresponding subsystem:

$$\begin{aligned}
\rho_{\mathbb{Q}_{\mathbb{M}_{h\ldots1}}} &= \mathrm{Tr}_{(\mathbb{Q}_{\mathbb{M}_h}\mathbb{Q}_{\mathbb{M}_{(h-1)\ldots1}})}\left(U_C|0\rangle^{\otimes n}\langle 0|^{\otimes n} \otimes \rho_{\mathbb{Q}_{\mathbb{M}_h}} \otimes \rho_{\mathbb{Q}_{\mathbb{M}_{(h-1)\ldots1}}}U_C^\dagger\right) \\
&= \sum_{\psi_t \subseteq \Phi} \sum_{\cap\psi_j = \psi_t} \prod_{1 \le h \le k} \left|\varphi_h(\psi_j)e^{i\theta_h(\psi_j)}\right|^2 |\psi_t\rangle\langle\psi_t| \\
&= \sum_{\psi_t \subseteq \Phi} \sum_{\cap\psi_j = \psi_t} \prod_{1 \le h \le k} \left|\sqrt{m_h(\psi_j)}\right|^2 |\psi_t\rangle\langle\psi_t|,
\end{aligned} \tag{25}$$

where $|\psi_t\rangle$ is defined in Definition 13. When $h = k$, it indicates all the encoded quantum states corresponding to the BPAs are fused through the adaptive quantum circuit of DRC by $k-1$ U_C Toffoli gates. A total of $|0\rangle^{\otimes(2k-1)n}$ qubits are required to complete the DRC, where $|0\rangle^{\otimes kn}$ qubits are used for encoding the quantum states of the BPAs, and $|0\rangle^{\otimes(k-1)n}$ qubits are allocated as auxiliary qubits for storing the processed information.

3.3 Measurement in the adaptive quantum circuit for decision-making

We define two types of measurement operators in terms of the quantum basic probability level and the plausibility level decision-making for different application requirements.

3.3.1 Quantum measurement for quantum basic probability level decision-making

We first define a measurement operator for quantum basic probability level decision-making. After that, we define a QBP expression for quantum measurement outcomes. On this basis, we can measure the results from the adaptive quantum circuit of DRC.

Definition 15 (Measurement operator for quantum basic probability level decision-making)**.** *The measurement operator $\mathcal{M}_{QBP}$ is defined for the quantum basic probability level decision-making as:*

$$\mathcal{M}_{QBP} = \{\mathcal{M}_{|\psi_t\rangle} | \psi_t \subseteq \Phi\}, \quad \mathcal{M}_{|\psi_t\rangle} = |\psi_t\rangle\langle\psi_t|, \tag{26}$$

where $|\psi_t\rangle$ is defined in Definition 13.

Definition 16 (QBP expression for quantum measurement outcomes)**.** *Let $\rho_{\mathbb{Q}_{\mathbb{M}_{k\ldots1}}}$ be a density operator with regards to the trace of the output of U_C. Let $\mathcal{M}_{QBP} = \{\mathcal{M}_{|\psi_t\rangle} = |\psi_t\rangle\langle\psi_t| | \psi_t \subseteq \Phi\}$ be a set of measurement operators. The quantum basic probability (QBP) expression for quantum measurement outcomes is defined as:*

$$\mathrm{M}(\psi_t) = \frac{\mathrm{Tr}\left(\mathcal{M}^{\dagger}_{|\psi_t\rangle}\mathcal{M}_{|\psi_t\rangle} \cdot \rho_{\mathbb{Q}_{\mathbb{M}_{k\ldots1}}}\right)}{\sum\limits_{\substack{\psi_v \subseteq \Phi \\ \psi_v \neq \emptyset}} \mathrm{Tr}\left(\mathcal{M}^{\dagger}_{|\psi_v\rangle}\mathcal{M}_{|\psi_v\rangle} \cdot \rho_{\mathbb{Q}_{\mathbb{M}_{k\ldots1}}}\right)} = \frac{\sum\limits_{\cap\psi_j = \psi_t} \prod\limits_{1 \leq h \leq k} \left|\varphi_h(\psi_j) e^{i\theta_h(\psi_j)}\right|^2}{\sum\limits_{\substack{\psi_v \subseteq \Phi \\ \psi_v \neq \emptyset}} \sum\limits_{\cap\psi_j = \psi_v} \prod\limits_{1 \leq h \leq k} \left|\varphi_h(\psi_j) e^{i\theta_h(\psi_j)}\right|^2}, \tag{27}$$

which forms a quantum basic probability distribution (QBPD) M.

After implementing the measurement operator $\mathcal{M}_{QBP}$, for $\psi_t \subseteq \Phi, \psi_t \neq \emptyset$, because $\left|\varphi_h(\psi_j) e^{i\theta_h(\psi_j)}\right|^2 = \left|\sqrt{m_h(\psi_j)}\right|^2$ and $m(\psi_t) = \mathrm{M}(\psi_t)$, the combined BPA can be generated:

$$m(\psi_t) = \mathrm{M}(\psi_t) = \frac{\sum\limits_{\cap\psi_j = \psi_t} \prod\limits_{1 \leq h \leq k} \left|\sqrt{m_h(\psi_j)}\right|^2}{\sum\limits_{\substack{\psi_v \subseteq \Phi \\ \psi_v \neq \emptyset}} \sum\limits_{\cap\psi_j = \psi_v} \prod\limits_{1 \leq h \leq k} \left|\sqrt{m_h(\psi_j)}\right|^2}. \tag{28}$$

For $\psi_t = \emptyset$, we have

$$\begin{aligned} K &= \mathrm{Tr}\left(\mathcal{M}^{\dagger}_{|\emptyset\rangle}\mathcal{M}_{|\emptyset\rangle} \cdot \rho_{\mathbb{Q}_{\mathbb{M}_{k\ldots1}}}\right) \\ &= \sum_{\cap\psi_j = \emptyset} \prod_{1 \leq h \leq k} \left|\varphi_h(\psi_j) e^{i\theta_h(\psi_j)}\right|^2 = \sum_{\cap\psi_j = \emptyset} \prod_{1 \leq h \leq k} \left|\sqrt{m_h(\psi_j)}\right|^2. \end{aligned} \tag{29}$$

Then, for $\psi_t \subseteq \Phi, \psi_t \neq \emptyset$, we also have

$$m(\psi_t) = \frac{\mathrm{Tr}\left(\mathcal{M}^{\dagger}_{|\psi_t\rangle}\mathcal{M}_{|\psi_t\rangle} \cdot \rho_{\mathbb{Q}_{\mathbb{M}_{k\ldots1}}}\right)}{1 - \mathrm{Tr}\left(\mathcal{M}^{\dagger}_{|\emptyset\rangle}\mathcal{M}_{|\emptyset\rangle} \cdot \rho_{\mathbb{Q}_{\mathbb{M}_{k\ldots1}}}\right)} = \frac{\sum\limits_{\cap\psi_j = \psi_t} \prod\limits_{1 \leq h \leq k} \left|\sqrt{m_h(\psi_j)}\right|^2}{1 - K}. \tag{30}$$

When implementing AQC-DRC based on the quantum measurement for quantum basic probability level decision-making, denoted as AQC-DRC$_{\mathrm{QBP}}$, for $||\psi_t\rangle| = 1$, a decision can be made as follow:

$$w = \arg\max_t\{\mathrm{M}(\psi_t)\} = \arg\max_t\{m(\psi_t)\}, \quad \text{and} \quad D = \psi_w. \tag{31}$$

3.3.2 Quantum measurement for quantum plausibility level decision-making

Starting from the density matrix $\rho_{\mathbb{Q}_{\mathbb{M}_{h\ldots1}}}$, we perform a partial trace over the auxiliary $(n-1)$ qubits $\{q_n \ldots q_{w+1} q_{w-1} \ldots q_1\}$ using $\mathrm{Tr}_{(q_n \ldots q_{w+1} q_{w-1} \ldots q_1)}$. This yields the reduced density matrix

$\rho^{w}_{\mathbb{Q}_{\mathbb{M}_{h\ldots1}}}$, which describes the state associated with the w-th qubit:

$$\begin{aligned}
&\rho^{w}_{\mathbb{Q}_{\mathbb{M}_{h\ldots1}}} = \mathrm{Tr}_{(q_n\ldots q_{w+1}q_{w-1}\ldots q_1)}\left(\rho_{\mathbb{Q}_{\mathbb{M}_{h\ldots1}}}\right)\\
&= \sum_{\phi_w\in\psi_t}\sum_{\cap\psi_j=\psi_t}\prod_{1\le h\le k}\left|\varphi_h(\psi_j)e^{i\theta_h(\psi_j)}\right|^2|1\rangle\langle1| + \left(1-\sum_{\phi_w\in\psi_t}\sum_{\cap\psi_j=\psi_t}\prod_{1\le h\le k}\left|\varphi_h(\psi_j)e^{i\theta_h(\psi_j)}\right|^2\right)|0\rangle\langle0|\\
&= \sum_{\phi_w\in\psi_t}\sum_{\cap\psi_j=\psi_t}\prod_{1\le h\le k}\left|\sqrt{m_h(\psi_j)}\right|^2|1\rangle\langle1| + \left(1-\sum_{\phi_w\in\psi_t}\sum_{\cap\psi_j=\psi_t}\prod_{1\le h\le k}\left|\sqrt{m_h(\psi_j)}\right|^2\right)|0\rangle\langle0|.
\end{aligned} \tag{32}$$

Definition 17 (Measurement operator for quantum plausibility level decision-making)**.** *The measurement operator $\mathcal{M}_{QPl}$ is defined for quantum plausibility level decision-making as:*

$$\mathcal{M}_{QPl} = \{\mathcal{M}_{|u\rangle}|u\in\{0,1\}\},\quad \mathcal{M}_{|u\rangle} = |u\rangle\langle u|. \tag{33}$$

Definition 18 (QPl expression for quantum measurement outcomes)**.** *Let $\rho^{w}_{\mathbb{Q}_{\mathbb{M}_{k\ldots1}}}$ be the density operator of the w-th qubit in terms of the output of U^C. Let $\mathcal{M}_{QPl} = \{\mathcal{M}_{|u\rangle} = |u\rangle\langle u||u\in\{0,1\}\}$ and $\mathcal{M}_{QBP} = \{\mathcal{M}_{|\psi_t\rangle} = |\psi_t\rangle\langle\psi_t||\psi_t\subseteq\Phi\}$ be a set of measurement operators. The quantum plausibility (QPl) expression for quantum measurement outcomes is defined as:*

$$\mathrm{QPl}(\psi_w) = \frac{\mathrm{Tr}\left(\mathcal{M}^{\dagger}_{|1\rangle}\mathcal{M}_{|1\rangle}\cdot\rho^{w}_{\mathbb{Q}_{\mathbb{M}_{k\ldots1}}}\right)}{1-\mathrm{Tr}\left(\mathcal{M}^{\dagger}_{|\emptyset\rangle}\mathcal{M}_{|\emptyset\rangle}\cdot\rho_{\mathbb{Q}_{\mathbb{M}_{k\ldots1}}}\right)} = \frac{\sum\limits_{\phi_w\in\psi_t}\sum\limits_{\cap\psi_j=\psi_t}\prod\limits_{1\le h\le k}\left|\varphi_h(\psi_j)e^{i\theta_h(\psi_j)}\right|^2}{1-K}. \tag{34}$$

After implementing the measurement operator $\mathcal{M}_{QPl}$, because $\left|\varphi_h(\psi_j)e^{i\theta_h(\psi_j)}\right|^2 = \left|\sqrt{m_h(\psi_j)}\right|^2$ and $\mathrm{Pl}(\psi_w) = \mathrm{QPl}(\phi_w)$ for each element ϕ_w $(1\le w\le n)$ in FOD, the Pl for ϕ_w can be generated:

$$\mathrm{Pl}(\phi_w) = \mathrm{QPl}(\phi_w) = \frac{\sum\limits_{\phi_w\in\psi_t}\sum\limits_{\cap\psi_j=\psi_t}\prod\limits_{1\le h\le k}\left|\sqrt{m_h(\psi_j)}\right|^2}{1-K}. \tag{35}$$

Since $1/(1-K)$ is a constant normalization factor, it does not affect the decision-making outcome, and we can simply Eq. (34) for decision-making to improve computational efficiency witout loss of generality:

$$\widehat{\mathrm{QPl}}(\psi_w) = \mathrm{Tr}\left(\mathcal{M}^{\dagger}_{|1\rangle}\mathcal{M}_{|1\rangle}\cdot\rho^{w}_{\mathbb{Q}_{\mathbb{M}_{k\ldots1}}}\right). \tag{36}$$

When implementing AQC-DRC based on the quantum plausibility level decision-making, denoted as AQC-DRC$_{\mathrm{QPl}}$, a decision can be made as follow:

$$w = \arg\max_{w}\{\widehat{\mathrm{QPl}}(\phi_w)\} = \arg\max_{w}\{\mathrm{Pl}(\phi_w)\},\quad \text{and}\quad D = \phi_w. \tag{37}$$

Therefore, based on the definitions and rigorous mathematical derivations in Sections 3.1-3.3, we can observe that the proposed AQC-DRC$_{\mathrm{QBP}}$ yields results consistent with DRC at the quantum basic probability level, while AQC-DRC$_{\mathrm{QPl}}$ aligns with DRC+QPl at the quantum plausibility level. These results demonstrate deterministic computation and guarantee that no information is lost.

4 Application in pattern classification

In the experimental setup, three distinct datasets namely Iris (Ir), Abalone (Ab), and Knowledge (Kn) are chosen from the UCI repository (https://archive.ics.uci.edu/). For the Iris dataset, all attributes and classes are selected. Whereas, due to the limitation of available qubits, for the Abalone dataset, we randomly select five attributes (Length, Diameter, Height, Whole_weight, and Viscera_weight) and two classes (Rings = 5 and Rings = 15); for the Knowledge dataset, all classes are selected, but three attributes (STR, LPR, and PEG) are randomly select. The details of each dataset, including the selected attributes and classes, are summarized in Table 1. The approach from [66] is adopted to generate the BPA for each attribute. The individual BPAs of each dataset are

subsequently aggregated to perform classification using different methods. To evaluate the effectiveness of the proposed methods, we compare the classical DRC [11], DRC+QPl, QC-DRC$_{\text{QBP}}$ [62], QC-DRC$_{\text{QBP}}$+QPl (the QC-DRC$_{\text{QBP}}$ is used firstly to obtain the QBP, and then to combine the QBP into the QPl using the classical process), and the proposed AQC-DRC$_{\text{QBP}}$, AQC-DRC$_{\text{QBP}}$+QPl (the AQC-DRC$_{\text{QBP}}$ is used firstly to obtain the QBP, and then to combine the QBP into the QPl using the classical process) and AQC-DRC$_{\text{QPl}}$ based on the average accuracy (Acc) obtained from κ-fold cross-validation ($\kappa = 5$). To analyze the robustness of different methods, we further evaluate the average accuracy performance of each method under varying numbers of measurement shots (s).

Table 1: Dataset information

	Ir	Ab	Kn
# Class	3	2	4
# Attribute	4	5	3
# Instance	150	218	403

Table 2: Computational complexity analysis

Method	Complexity	Qubits
DRC	$O(kN2^{2n})$	/
DRC + QPl	$O(kN2^{2n})$	/
QC-DRC$_{\text{QBP}}$	$O(kn + kN)$	$3n$
QC-DRC$_{\text{QBP}}$ + QPl	$O(kn + kN + nN)$	$3n$
AQC-DRC$_{\text{QBP}}$	$O(kn + N)$	$(2k-1)n$
AQC-DRC$_{\text{QBP}}$ + QPl	$O(kn + nN)$	$(2k-1)n$
AQC-DRC$_{\text{QPl}}$	$O(kn^2)$	$(2k-1)n$

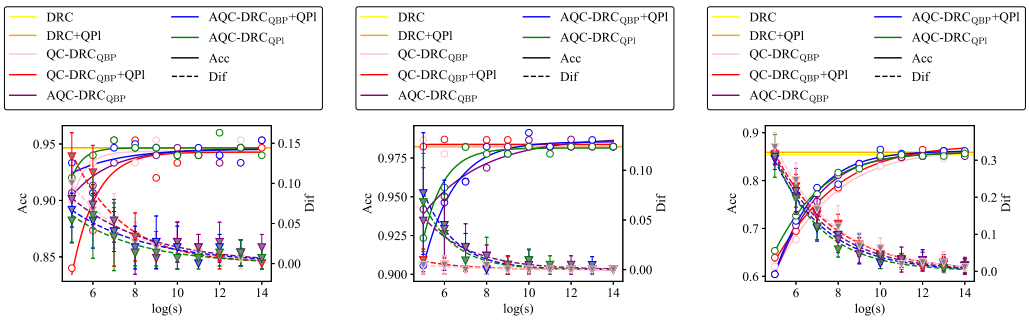

(a) Iris. (b) Abalone. (c) Knowledge.

Figure 2: Comparison of the classical and quantum methods in terms of Acc and Dif metrics.

The experimental results are displayed in Fig. 2 and Tables A1-A6. It is observed that as the number of shots s increases from 2^5 to 2^6, 2^7, 2^8, 2^9, 2^{10}, 2^{11}, 2^{12}, 2^{13}, and finally 2^{14}, for Iris dataset, the average accuracies of QC-DRC$_{\text{QBP}}$ change as follows: 0.9, 0.9333, 0.9467, 0.9333, 0.9533, 0.9333, 0.9467, 0.9333, 0.9533, and 0.9467; the average accuracies of QC-DRC$_{\text{QBP}}$+QPl change as follows: 0.9333, 0.9067, 0.9467, 0.95, 0.9467, 0.94, 0.9467, 0.94, 0.9333, and 0.9533; the average accuracies of AQC-DRC$_{\text{QBP}}$ change as follows: 0.9067, 0.9133, 0.9333, 0.9467, 0.94, 0.9467, 0.94, 0.9333, 0.9467, and 0.9533; the average accuracies of AQC-DRC$_{\text{QBP}}$+QPl change as follows: 0.92, 0.94, 0.9533, 0.9467, 0.9467, 0.94, 0.94, 0.96, 0.9467, and 0.94; the average accuracies of AQC-DRC$_{\text{QPl}}$ change as follows: 0.84, 0.8733, 0.9533, 0.9533, 0.92, 0.9333, 0.94, 0.94, 0.9467, and 0.9467. While the classical DRC and DRC+QPl maintain an average accuracy of 0.9467, the accuracies of QC-DRC$_{\text{QBP}}$, QC-DRC$_{\text{QBP}}$+QPl, the proposed AQC-DRC$_{\text{QBP}}$, AQC-DRC$_{\text{QBP}}$+QPl, and AQC-DRC$_{\text{QPl}}$ gradually approach those of the classical models. Similarly, on the Abalone dataset, classical DRC and DRC+QPl achieve accuracies of 0.9823; on the Knowledge dataset, they reach 0.8539 and 0.8591, respectively. The corresponding quantum methods, including QC-DRC$_{\text{QBP}}$, QC-DRC$_{\text{QBP}}$+QPl, AQC-DRC$_{\text{QBP}}$+QPl, and AQC-DRC$_{\text{QPl}}$, also demonstrate a consistent trend of converging toward the classical models' performance.

On the other hand, we define an evaluation metric, Dif, to quantify the difference between the classification results of the classical DRC, and those produced by the QC-DRC$_{\text{QBP}}$, QC-DRC$_{\text{QBP}}$+QPl, the proposed AQC-DRC$_{\text{QBP}}$, AQC-DRC$_{\text{QBP}}$+QPl, and AQC-DRC$_{\text{QPl}}$. The metric Dif$_s$ under different numbers of shots s for k-fold cross-validation is defined as:

$$\text{Dif}_s\left(\frac{\text{Method}}{\text{DRC}}\right) = \frac{1}{5}\sum_{\kappa=1}^{5}\frac{|\text{Mc}_s^{\kappa}(\text{Method}) \cup \text{Mc}^{\kappa}(\text{DRC}) - \text{Mc}_s^{\kappa}(\text{Method}) \cap \text{Mc}^{\kappa}(\text{DRC})|}{|\text{Tc}^{\kappa}|}, \quad (38)$$

where Mc_s^{κ}(Method) denotes the misclassified instances by other methods, including QC-DRC$_{\mathrm{QBP}}$, QC-DRC$_{\mathrm{QBP}}$+QPl, the proposed AQC-DRC$_{\mathrm{QBP}}$, AQC-DRC$_{\mathrm{QBP}}$+QPl, and AQC-DRC$_{\mathrm{QPl}}$; Mc^{κ}(DRC) represents the misclassified instances by the classical DRC; Tc^{κ} denotes the test instances in the κ-th fold of cross-validation; and $|\cdot|$ represents the number of instances. StD denotes the standard deviation of Dif_s with respect to κ-fold cross-validation. The experimental results are displayed in Fig. 2 and Tables A7-A12. It is observed that as the number of shots s increases from 2^5 to 2^{14}, the Dif values of the QC-DRC$_{\mathrm{QBP}}$, QC-DRC$_{\mathrm{QBP}}$+QPl, the proposed AQC-DRC$_{\mathrm{QBP}}$, AQC-DRC$_{\mathrm{QBP}}$+QPl, and AQC-DRC$_{\mathrm{QPl}}$ relative to the classical DRC gradually converge to zero in terms of three distinct datasets.

5 Computational complexity analysis

Assume that there are n elements in the frame of discernment (FOD) and k pieces of evidence, with a total of N focal elements. As shown in Table 2, the time complexities of the classical DRC and DRC+QPl are $O(kN2^{2n})$. In contrast, with sufficient auxiliary qubits, the time complexities of QC-DRC$_{\mathrm{QBP}}$, QC-DRC$_{\mathrm{QBP}}$+QPl, AQC-DRC$_{\mathrm{QBP}}$, AQC-DRC$_{\mathrm{QBP}}$+QPl and AQC-DRC$_{\mathrm{QPl}}$, in terms of both the circuit depth and the normalization process, are $O(kn + kN)$, $O(kn + kN + nN)$, $O(kn + N)$, $O(kn + nN)$ and $O(kn^2)$, respectively. Comparative analysis reveals that QC-DRC$_{\mathrm{QBP}}$, QC-DRC$_{\mathrm{QBP}}$+QPl, AQC-DRC$_{\mathrm{QBP}}$, AQC-DRC$_{\mathrm{QBP}}$+QPl and AQC-DRC$_{\mathrm{QPl}}$ all achieve exponential reductions in time complexity relative to the classical DRC and DRC+QPl. Notably, AQC-DRC$_{\mathrm{QBP}}$ improves upon QC-DRC$_{\mathrm{QBP}}$ by reducing the time complexity by $(k-1)N$; AQC-DRC$_{\mathrm{QBP}}$+QPl improves upon QC-DRC$_{\mathrm{QBP}}$+QPl by reducing the time complexity by kN. Furthermore, since $1 \leq N \leq 2^n$, when $N = 2^n$, AQC-DRC$_{\mathrm{QPl}}$ achieves an exponential improvement over QC-DRC$_{\mathrm{QBP}}$, QC-DRC$_{\mathrm{QBP}}$+QPl, AQC-DRC$_{\mathrm{QBP}}$ and AQC-DRC$_{\mathrm{QBP}}$+QPl. Regarding space complexity, QC-DRC$_{\mathrm{QBP}}$, QC-DRC$_{\mathrm{QBP}}$+QPl require $3n$ qubits. In comparison, AQC-DRC$_{\mathrm{QBP}}$, AQC-DRC$_{\mathrm{QBP}}$+QPl and AQC-DRC$_{\mathrm{QPl}}$ require $(2k-1)n$ qubits, growing linearly with both the number of elements n in the FOD and the number of evidence sources k. The results indicate that the proposed AQC-DRC$_{\mathrm{QBP}}$, AQC-DRC$_{\mathrm{QBP}}$+QPl and AQC-DRC$_{\mathrm{QPl}}$ exhibit superior time complexity compared to existing approaches. Specifically, AQC-DRC$_{\mathrm{QPl}}$ demonstrates optimal performance as N tends toward 2^n. A detailed analysis can be found in Appendix A1.

6 Limitation and conclusion

In this paper, to address efficient classification under uncertain environments, we propose an adaptive quantum circuit for Dempster's rule of combination (AQC-DRC) to support quantum basic probability and plausibility level decision-making within the framework of quantum evidence theory (QET). The AQC-DRC, as a generalized quantum Bayesian inference method, enables deterministic computation of DRC, ensuring that quantum fusion outcomes in uncertain pattern classification are fully consistent with those of the classical method. Furthermore, it achieves an exponential reduction in computational complexity, positioning it as a promising approach for real-time quantum multisource information fusion. The architecture of the proposed AQC-DRC is conceptually straightforward and highly scalable, which facilitates its practical implementation. It is observed that the quantum basic probability amplitude function in QET can naturally express the quantum amplitude encoding. The quantum basic probability in QET, forming the quantum basic probability distribution, can directly express quantum measurement outcomes for basic probability level decision-making, while the quantum plausibility function in QET can also naturally represent the quantum measurement outcomes for plausibility-level decision-making. These insights not only broaden the understanding of QET, but also provide a more intuitive physical interpretation of quantum amplitude encoding and quantum measurement outcomes.

However, this study revealed that the current version of AQC-DRC is unable to process complex-valued input data, thereby constraining its applicability. Future research will focus on extending AQC-DRC's capabilities through further developments in quantum computing techniques. Notably, Xu et al. [67] proposed a multimodal optimization strategy, which is an excellent strategy to enhance the complementarity of multimodal data and obtain preferable classification results. Consequently, this work holds the potential to incorporate such strategies to establish a trustworthy fusion and decision-making framework for handling heterogeneous data in future applications.

Acknowledgments

The authors greatly appreciate the reviewers' suggestions and the area chair's encouragement. This research is supported by the National Natural Science Foundation of China (No. 62473067), Xiaomi Young Talents Program, Chongqing Talents: Exceptional Young Talents Project (No. cstc2022ycjh-bgzxm0070), and Chongqing Overseas Scholars Innovation Program (No. cx2022024).

References

[1] Yasin Abbasi Yadkori, Ilja Kuzborskij, András György, and Csaba Szepesvari. To believe or not to believe your LLM: Iterative prompting for estimating epistemic uncertainty. *Advances in Neural Information Processing Systems*, 37:58077–58117, 2024.

[2] Zhiyuan Hu, Chumin Liu, Xidong Feng, Yilun Zhao, See-Kiong Ng, Anh Tuan Luu, Junxian He, Pang Wei W Koh, and Bryan Hooi. Uncertainty of thoughts: Uncertainty-aware planning enhances information seeking in LLMs. *Advances in Neural Information Processing Systems*, 37:24181–24215, 2024.

[3] Joel Weijia Lai, Candice Ke En Ang, U Rajendra Acharya, and Kang Hao Cheong. Schizophrenia: a survey of artificial intelligence techniques applied to detection and classification. *International Journal of Environmental Research and Public Health*, 18(11):6099, 2021.

[4] You HE, Yu LIU, Yaowen LI, Ziran DING, Kai DONG, Yaqi CUI, Caisheng ZHANG, Xueqian WANG, Zhi LI, and Chen GUO. Development and prospects of multisource information fusion. *Acta Aeronautica et Astronautica Sinica*, 46(6), 2025.

[5] Zhen Wang, Chunjiang Mu, Shuyue Hu, Chen Chu, and Xuelong Li. Modelling the dynamics of regret minimization in large agent populations: a master equation approach. In *The 31st International Joint Conference on Artificial Intelligence, (IJCAI-22)*, pages 534–540, 2022.

[6] Xinde Li, Dunkin Fir, and Dezert Jean. Multi-source information fusion: Progress and future. *Chinese Journal of Aeronautics*, 37(7):24–58, 2024.

[7] Tangfan Xiahou, Zhiguo Zeng, Yu Liu, and Hong-Zhong Huang. Measuring conflicts of multisource imprecise information in multistate system reliability assessment. *IEEE Transactions on Reliability*, 71(4):1417–1434, 2021.

[8] Ruijie Liu, Tangfan Xiahou, and Yu Liu. Multisource imprecise information calibration for reliability assessment of multistate systems: A consensus reaching perspective. *IEEE Transactions on Reliability*, 74(1):2226–2240, 2025.

[9] Chenghai Li, Ke Wang, Yafei Song, Peng Wang, and Lemin Li. Air target intent recognition method combining graphing time series and diffusion models. *Chinese Journal of Aeronautics*, page DOI: 10.1016/j.cja.2024.08.008, 2024.

[10] Fu Wang, Tangfan Xiahou, Xian Zhang, Pan He, Taibo Yang, Jiang Niu, Caixue Liu, and Yu Liu. Convolutional preprocessing transformer-based fault diagnosis for rectifier-filter circuits in nuclear power plants. *Reliability Engineering & System Safety*, 249:110198, 2024.

[11] Arthur P Dempster. Upper and lower probability inferences for families of hypotheses with monotone density ratios. *The Annals of Mathematical Statistics*, pages 953–969, 1969.

[12] Glenn Shafer. *A mathematical theory of evidence*, volume 42. Princeton University Press, 1976.

[13] Jian-Bo Yang and Dong-Ling Xu. Maximum likelihood evidential reasoning. *Artificial Intelligence*, 340:104289, 2025.

[14] Chao Fu, Bingbing Hou, Min Xue, Leilei Chang, and Weiyong Liu. Extended belief rule-based system with accurate rule weights and efficient rule activation for diagnosis of thyroid nodules. *IEEE Transactions on Systems, Man, and Cybernetics: Systems*, 53(1):251–263, 2023.

[15] Xinyang Deng and Wen Jiang. A framework for the fusion of non-exclusive and incomplete information on the basis of D number theory. *Applied Intelligence*, 53:11861–11884, 2023.

[16] You Cao, Zhijie Zhou, Shuaiwen Tang, Pengyun Ning, and Manlin Chen. On the robustness of belief-rule-based expert systems. *IEEE Transactions on Systems, Man, and Cybernetics: Systems*, 53(10):6043–6055, 2023.

[17] Fuyuan Xiao, Junhao Wen, Witold Pedrycz, and Masayoshi Aritsugi. Complex evidence theory for multisource data fusion. *Chinese Journal of Information Fusion*, 1(2):134–159, 2024.

[18] Yong Deng. Random permutation set. *International Journal of Computers Communications & Control*, 17(1):4542, 2022.

[19] Jixiang Deng, Yong Deng, and Jian-Bo Yang. Random permutation set reasoning. *IEEE Transactions on Pattern Analysis and Machine Intelligence*, page DOI: 10.1109/TPAMI.2024.3438349, 2024.

[20] Qianli Zhou, Witold Pedrycz, and Yong Deng. Order-2 probabilistic information fusion on random permutation set. *IEEE Transactions on Knowledge and Data Engineering*, page 10.1109/TKDE.2024.3484009, 2024.

[21] Yidan Wang, Zhen Li, and Yong Deng. A new orthogonal sum in random permutation set. *Fuzzy Sets and Systems*, 490:109034, 2024.

[22] Jiefeng Zhou, Zhen Li, and Yong Deng. Random walk in random permutation set theory. *Chaos: An Interdisciplinary Journal of Nonlinear Science*, 34(9):093137, 2024.

[23] Fuyuan Xiao. Quantum X-entropy in generalized quantum evidence theory. *Information Sciences*, 643:119177, 2023.

[24] Fuyuan Xiao. Quantum evidence theory. *viXra:2504.0202, https://rxiv.org/abs/2504.0202*.

[25] Mingli Lei and Kang Hao Cheong. Node influence ranking in complex networks: A local structure entropy approach. *Chaos, Solitons & Fractals*, 160:112136, 2022.

[26] Zhen Wang, Lin Wang, Attila Szolnoki, and Matjaž Perc. Evolutionary games on multilayer networks: a colloquium. *The European physical journal B*, 88:1–15, 2015.

[27] Zhen Wang, Satoshi Kokubo, Marko Jusup, and Jun Tanimoto. Universal scaling for the dilemma strength in evolutionary games. *Physics of life reviews*, 14:1–30, 2015.

[28] Bo Cao, Chenghai Li, Yafei Song, Yueyi Qin, and Chen Chen. Network intrusion detection model based on CNN and GRU. *Applied Sciences*, 12(9):4184, 2022.

[29] Junhao Yu, Fuyuan Xiao, Yi Zhang, Zehong Cao, and Chin-Teng Lin. A CDGFN-based quantum multisource information fusion with its application in time series classification. *IEEE Transactions on Knowledge and Data Engineering*, page DOI: 10.1109/TKDE.2026.3652983, 2026.

[30] Zhun-Ga Liu, Guang-Hui Qiu, Shu-Yue Wang, Tian-Cheng Li, and Quan Pan. A new belief-based bidirectional transfer classification method. *IEEE Transactions on Cybernetics*, 52(8):8101–8113, 2021.

[31] Xuelong Li, Marko Jusup, Zhen Wang, Huijia Li, Lei Shi, Boris Podobnik, H Eugene Stanley, Shlomo Havlin, and Stefano Boccaletti. Punishment diminishes the benefits of network reciprocity in social dilemma experiments. *Proceedings of the National Academy of Sciences*, 115(1):30–35, 2018.

[32] Zhen Wang, Marko Jusup, Lei Shi, Joung-Hun Lee, Yoh Iwasa, and Stefano Boccaletti. Exploiting a cognitive bias promotes cooperation in social dilemma experiments. *Nature Communications*, 9(1):2954, 2018.

[33] Zhen Wang, Marko Jusup, Rui-Wu Wang, Lei Shi, Yoh Iwasa, Yamir Moreno, and Jürgen Kurths. Onymity promotes cooperation in social dilemma experiments. *Science Advances*, 3(3):e1601444, 2017.

[34] Shiyuan Yang, Debiao Meng, Hongtao Wang, and Chang Yang. A novel learning function for adaptive surrogate-model-based reliability evaluation. *Philosophical Transactions of the Royal Society A*, 382(2264):20220395, 2024.

[35] Xinyang Deng, Xiang Li, and Wen Jiang. Evidence representation of uncertain information on a frame of discernment with semantic association. *Information Fusion*, 111:Article ID 102538, 2024.

[36] Tong Zhao, Zhen Li, and Yong Deng. Linearity in Deng entropy. *Chaos, Solitons & Fractals*, 178:114388, 2024.

[37] Tianxiang Zhan, Jiefeng Zhou, Zhen Li, and Yong Deng. Generalized information entropy and generalized information dimension. *Chaos, Solitons & Fractals*, 184:114976, 2024.

[38] Fuyuan Xiao, Weiping Ding, and Witold Pedrycz. A generalized f-divergence with applications in pattern classification. *IEEE Transactions on Knowledge and Data Engineering*, page DOI: 10.1109/TKDE.2025.3530524, 2025.

[39] Bingyi Kang and Chunjiang Zhao. Deceptive evidence detection in information fusion of belief functions based on reinforcement learning. *Information Fusion*, 103:102102, 2024.

[40] Yingcheng Huang, Fuyuan Xiao, Zehong Cao, and Chin-Teng Lin. Higher order fractal belief Rényi divergence with its applications in pattern classification. *IEEE Transactions on Pattern Analysis and Machine Intelligence*, 45(12):14709–14726, 2023.

[41] Yingcheng Huang, Fuyuan Xiao, Zehong Cao, and Chin-Teng Lin. Fractal belief Rényi divergence with its applications in pattern classification. *IEEE Transactions on Knowledge and Data Engineering*, 36(12):8297–8312, 2024.

[42] Ling Huang, Su Ruan, Pierre Decazes, and Thierry Denœux. Deep evidential fusion with uncertainty quantification and reliability learning for multimodal medical image segmentation. *Information Fusion*, 113:102648, 2025.

[43] Lang Zhang and Fuyuan Xiao. Belief Rényi divergence of divergence and its application in time series classification. *IEEE Transactions on Knowledge and Data Engineering*, 36(8):3670–3681, 2024.

[44] Mi Zhou, Ya-Qian Zheng, Yu-Wang Chen, Ba-Yi Cheng, Enrique Herrera-Viedma, and Jian Wu. A large-scale group consensus reaching approach considering self-confidence with two-tuple linguistic trust/distrust relationship and its application in life cycle sustainability assessment. *Information Fusion*, 94:181–199, 2023.

[45] Deqiang Han, Jean Dezert, and Zhansheng Duan. Evaluation of probability transformations of belief functions for decision making. *IEEE Transactions on Systems, Man, and Cybernetics: Systems*, 46(1):93–108, 2015.

[46] Liguo Fei, Xiaoyu Liu, and Changping Zhang. An evidential linguistic ELECTRE method for selection of emergency shelter sites. *Artificial Intelligence Review*, 57(4):81, 2024.

[47] Zhihui Xu Xiaoyan Su, Ziying Hong and Hong Qian. An improved cream model based on deng entropy and evidence distance. *Nuclear Engineering and Technology*, page DOI: 10.1016/j.net.2025.103485, 2025.

[48] Xingyuan Chen and Yong Deng. Evidential software risk assessment model on ordered frame of discernment. *Expert Systems with Applications*, 250:123786, 2024.

[49] Ya-Jing Zhou, Mi Zhou, Xin-Bao Liu, Ba-Yi Cheng, and Enrique Herrera-Viedma. Consensus reaching mechanism with parallel dynamic feedback strategy for large-scale group decision making under social network analysis. *Computers & Industrial Engineering*, 174:108818, 2022.

[50] Liguo Fei and Yanqing Wang. An optimization model for rescuer assignments under an uncertain environment by using Dempster–Shafer theory. *Knowledge-Based Systems*, 255:109680, 2022.

[51] Daniel Hothem, Ashe Miller, and Timothy Proctor. What is my quantum computer good for? quantum capability learning with physics-aware neural networks. *Advances in Neural Information Processing Systems*, 37:34846–34869, 2024.

[52] Po-Wei Huang and Patrick Rebentrost. Quantum algorithm for large-scale market equilibrium computation. *Advances in Neural Information Processing Systems*, 37:10878–10907, 2024.

[53] Baiyu Su and Qiang Liu. Quadratic quantum variational monte carlo. *Advances in Neural Information Processing Systems*, 37:22154–22177, 2024.

[54] Philipp Schleich, Marta Skreta, Lasse Kristensen, Rodrigo Vargas-Hernandez, and Alán Aspuru-Guzik. Quantum deep equilibrium models. *Advances in Neural Information Processing Systems*, 37:31940–31967, 2024.

[55] Leo Zhou, Joao Basso, and Song Mei. Statistical estimation in the spiked tensor model via the quantum approximate optimization algorithm. *Advances in Neural Information Processing Systems*, 37:28537–28588, 2024.

[56] Dar Gilboa, Hagay Michaeli, Daniel Soudry, and Jarrod McClean. Exponential quantum communication advantage in distributed inference and learning. *Advances in Neural Information Processing Systems*, 37:30425–30473, 2024.

[57] Mariia Baidachna, Rey Guadarrama, Gopal Ramesh Dahale, Tom Magorsch, Isabel Pedraza, Konstantin T Matchev, Katia Matcheva, Kyoungchul Kong, and Sergei Gleyzer. Quantum diffusion model for quark and gluon jet generation. In *Proceedings of the AAAI Symposium Series*, volume 7, pages 323–329, 2025.

[58] Connor Clayton, Jiaqi Leng, Gengzhi Yang, Yi-Ling Qiao, Ming Lin, and Xiaodi Wu. Differentiable quantum computing for large-scale linear control. *Advances in Neural Information Processing Systems*, 37:37176–37212, 2024.

[59] Chengchang Liu, Chaowen Guan, Jianhao He, and John Lui. Quantum algorithms for non-smooth non-convex optimization. *Advances in Neural Information Processing Systems*, 37:35288–35312, 2024.

[60] Xinyang Deng, Siyu Xue, and Wen Jiang. A novel quantum model of mass function for uncertain information fusion. *Information Fusion*, 89:619–631, 2023.

[61] Kim Nicoli, Christopher J Anders, Lena Funcke, Tobias Hartung, Karl Jansen, Stefan Kühn, Klaus-Robert Müller, Paolo Stornati, Pan Kessel, and Shinichi Nakajima. Physics-informed bayesian optimization of variational quantum circuits. *Advances in Neural Information Processing Systems*, 36:18341–18376, 2023.

[62] Huaping He and Fuyuan Xiao. A novel quantum Dempster's rule of combination for pattern classification. *Information Sciences*, page DOI: 10.1016/j.ins.2024.120617, 2024.

[63] Chenhui Qiang, Yong Deng, and Kang Hao Cheong. Information fractal dimension of mass function. *Fractals*, 30:2250110, 2022.

[64] Meizhu Li, Linshan Li, and Qi Zhang. A new distance measure between two basic probability assignments based on penalty coefficient. *Information Sciences*, page 120883, 2024.

[65] Li Zhu, Qianli Zhou, Yong Deng, and Kang Hao Cheong. Fractal-based basic probability assignment: A transient mass function. *Information Sciences*, 652:119767, 2024.

[66] Wen Jiang, Jun Zhan, Deyun Zhou, and Xin Li. A method to determine generalized basic probability assignment in the open world. *Mathematical Problems in Engineering*, 2016(1):3878634, 2016.

[67] Zhengyi Xu, Wen Jiang, and Jie Geng. Dual-branch dynamic modulation network for hyperspectral and lidar data classification. *IEEE Transactions on Geoscience and Remote Sensing*, 61:1–13, 2023.

Appendix

A1 Computational complexity analysis

All algorithms in Table 2 can be divided into two parts: the combination process, which involves obtaining the complete combined evidence or QPl; and the decision-making process, which involves using the obtained evidence or QPl to reach a decision. Assume that there are n elements in the frame of discernment (FOD) and k pieces of evidence, with a total of N focal elements.

1) DRC: When combining two pieces of evidence, the computational complexity of computing any of the focal elements is $O(2^{2n})$. Since there are N focal elements in total, the computational complexity of getting the complete combination result is $O(N2^{2n})$. The total number of combinations is $k-1$, so the total complexity of combination process is $O(kN2^{2n})$. After the combination process, a decision is made from n elements in the FOD. The computational complexity of the decision-making process is $O(n)$. Thus, the total computational complexity of DRC is $O(kN2^2n)$. ($O(kN2^{2n}+n)=O(kN2^{2n})$)

2) DRC+QPl: The computational complexity required to compute the QPl of a focal element from QBP in the classical process is $O(N)$. In the experimental process we made the decision to use the QPl of elements in FOD, so the computational complexity to compute QPl is $O(nN)$. Since the computational complexity of the DRC is $O(kN2^{2n})$, the total computational complexity of combination process is $O(kN2^{2n})$. ($O(kN2^{2n}+nN)=O(kN2^{2n})$, as $nN<kN2^{2n}$ when $n\geq 2$). The computational complexity of decision-making process is $O(n)$. Thus, the total computational complexity of DRC+QPl is $O(kN2^{2n})$.

3) QC-$\mathrm{DRC_{QBP}}$: The computational complexity of the quantum line part we use the depth of the quantum circuit to denote. The QC-$\mathrm{DRC_{QBP}}$ can only combine two pieces of evidence at a time. For the combination of two evidences the number of Toffoli gates used is n, so the computational complexity of the quantum circuit part is $O(n)$. There are N measurements obtained from quantum circuit, each of which requires a normalization process of complexity $O(1)$, so the computational complexity of the normalization part is $O(N)$. The computational complexity of two evidence combinations is $O(n+N)$. In total, $k-1$ combinations have to be performed, so the computational complexity of combination process is $O(kn+kN)$. The computational complexity of decision-making process is $O(n)$. Thus, the total computational complexity of QC-$\mathrm{DRC_{QBP}}$ is $O(kn+kN)$.

4) QC-$\mathrm{DRC_{QBP}}$+QPl: The computational complexity of QC-$\mathrm{DRC_{QBP}}$ is $O(kn+kN)$, and the computational complexity of the classical process of generating QPl from QBP is $O(nN)$. Therefore, the total computational complexity of combination process is $O(kn+kN+nN)$. The computational complexity of decision-making process is $O(n)$. Thus, the total computational complexity of QC-$\mathrm{DRC_{QBP}}$+QPl is $O(kn+kN+nN)$.

5) AQC-$\mathrm{DRC_{QBP}}$: The AQC-$\mathrm{DRC_{QBP}}$ can combine more than one piece of evidence at a time and the number required Toffoli (CCNOT) gate is $(k-1)n$. Thus, the complexity of the quantum circuit is $O(kn)$. The complexity of the normalization part is consistent with QC-$\mathrm{DRC_{QBP}}$ and is $O(N)$. Thus the total computational complexity of combination process is $O(kn+N)$. The computational complexity of decision-making process is $O(n)$. Thus, the total computational complexity of AQC-$\mathrm{DRC_{QBP}}$ is O(kn+N).

6) AQC-$\mathrm{DRC_{QBP}}$+QPl: The computational complexity of AQC-$\mathrm{DRC_{QBP}}$ is $O(kn+N)$, and the computational complexity of the classical process of generating QPl from QBP is $O(nN)$. Therefore, the total computational complexity of combination process is $O(kn+nN)$. ($O(kn+N+nN)=O(kn+(n+1)N)=O(kn+nN)$). The computational complexity of decision-making process is $O(n)$. Thus, the total computational complexity of AQC-$\mathrm{DRC_{QBP}}$+QPl is $O(kn+nN)$.

7) AQC-$\mathrm{DRC_{QPl}}$: The algorithm involves measuring n qubits individually, so a total of n quantum circuits are needed to complete it. The computational complexity of each of these quantum circuits is consistent with that of the quantum circuit of AQC-$\mathrm{DRC_{QBP}}$, which is $O(kn)$, and thus its total computational complexity of all quantum circuits is $O(kn^2)$. The computational complexity of decision-making process is $O(n)$. Thus, the total computational complexity of AQC-$\mathrm{DRC_{QPl}}$ is $O(kn^2)$.

A2 Experimental environment

The classical DRC and DRC+QPl methods were executed using Python 3.8.20 on a Windows 10 system equipped with a 13th Gen Intelő Core i9-13900K CPU (3.00 GHz), 128 GB RAM, and an NVIDIA GeForce RTX 4090 GPU. The quantum methods, including QC-DRCQBP, QC-DRCQBP+QPl, the proposed AQC-DRCQBP, AQC-DRCQBP+QPl, and AQC-DRC$_{\mathrm{QPl}}$, were mainly executed on the IonQ quantum simulator (https://ionq.com/).

A3 Experimental results

Table A1: Comparison of classification accuracies under κ-th fold of cross-validation for Iris dataset in terms of classical/quantum basic probability level decision-making.

Method	Shots	κ-th fold of cross-validation					Acc
		1	2	3	4	5	
DRC	–	1.0000	0.9000	0.9000	0.9667	0.9667	0.9467
QC-DRC$_{\mathrm{QBP}}$	32	0.9000	0.9333	0.8667	0.9000	0.9000	0.9000
	64	0.9333	0.9333	0.9333	0.9333	0.9333	0.9333
	128	1.0000	0.9333	0.9000	0.9333	0.9667	0.9467
	256	1.0000	0.9000	0.9333	0.9000	0.9333	0.9333
	512	1.0000	0.8667	0.9333	0.9667	1.0000	0.9533
	1024	1.0000	0.9000	0.9000	0.9333	0.9333	0.9333
	2048	1.0000	0.9333	0.8667	0.9667	0.9667	0.9467
	4096	1.0000	0.8667	0.9000	0.9333	0.9667	0.9333
	8192	1.0000	0.9000	0.9000	0.9667	1.0000	0.9533
	16384	1.0000	0.9000	0.9000	0.9667	0.9667	0.9467
AQC-DRC$_{\mathrm{QBP}}$	32	0.9000	0.8667	0.9000	0.9000	0.9667	0.9067
	64	0.9000	0.9333	0.8667	0.9000	0.9667	0.9133
	128	0.9667	0.9000	0.9333	0.9333	0.9333	0.9333
	256	1.0000	0.9000	0.9000	0.9667	0.9667	0.9467
	512	1.0000	0.9000	0.9000	0.9333	0.9667	0.9400
	1024	1.0000	0.9000	0.9333	0.9333	0.9667	0.9467
	2048	1.0000	0.8667	0.9333	0.9667	0.9333	0.9400
	4096	1.0000	0.8667	0.9000	0.9667	0.9333	0.9333
	8192	1.0000	0.8667	0.9000	0.9667	1.0000	0.9467
	16384	1.0000	0.8667	0.9333	0.9667	1.0000	0.9533

Table A2: Comparison of classification accuracies under κ-th fold of cross-validation for Iris dataset in terms of classical/quantum plausibility level decision-making.

Method	Shots	κ-th fold of cross-validation					Acc
		1	2	3	4	5	
DRC+QPl	–	1.0000	0.9000	0.9000	0.9667	0.9667	0.9467
QC-DRC$_{\mathrm{QBP}}$+QPl	32	0.9000	0.7333	0.8667	0.8000	0.9000	0.8400
	64	0.8667	0.8000	0.9000	0.8667	0.9333	0.8733
	128	1.0000	0.9333	0.9333	0.9667	0.9333	0.9533
	256	1.0000	0.9333	0.9000	0.9667	0.9667	0.9533
	512	1.0000	0.8667	0.8667	0.9333	0.9333	0.9200
	1024	1.0000	0.9000	0.9000	0.9333	0.9333	0.9333
	2048	1.0000	0.8667	0.9000	0.9333	1.0000	0.9400
	4096	1.0000	0.8667	0.9000	0.9667	0.9667	0.9400
	8192	1.0000	0.9000	0.8667	0.9667	1.0000	0.9467
	16384	1.0000	0.9000	0.9000	0.9667	0.9667	0.9467
AQC-DRC$_{\mathrm{QBP}}$+QPl	32	0.9667	0.9667	0.9000	0.9000	0.9333	0.9333
	64	0.9000	0.8333	0.9000	0.9333	0.9667	0.9067
	128	1.0000	0.9667	0.8667	0.9000	1.0000	0.9467
	256	1.0000	0.9000	0.9333	0.9600	0.9667	0.9500
	512	1.0000	0.9000	0.9000	0.9667	0.9667	0.9467
	1024	1.0000	0.8667	0.9000	0.9667	0.9667	0.9400
	2048	1.0000	0.9000	0.9000	0.9667	0.9667	0.9467
	4096	1.0000	0.8667	0.8667	0.9667	1.0000	0.9400
	8192	1.0000	0.8667	0.8667	0.9667	0.9667	0.9333
	16384	1.0000	0.9000	0.9333	0.9667	0.9667	0.9533
AQC-DRC$_{\mathrm{QPl}}$	32	0.9667	0.9333	0.8667	0.9000	0.9333	0.9200
	64	1.0000	0.9000	0.9000	0.9667	0.9333	0.9400
	128	1.0000	0.9333	0.9000	0.9667	0.9667	0.9533
	256	1.0000	0.9333	0.9000	0.9333	0.9667	0.9467
	512	1.0000	0.9333	0.9000	0.9333	0.9667	0.9467
	1024	1.0000	0.8667	0.9000	0.9667	0.9667	0.9400
	2048	1.0000	0.9000	0.8667	0.9667	0.9667	0.9400
	4096	1.0000	0.9333	0.9000	0.9667	1.0000	0.9600
	8192	1.0000	0.8667	0.9333	0.9667	0.9667	0.9467
	16384	1.0000	0.8667	0.9000	0.9667	0.9667	0.9400

Table A3: Comparison of classification accuracies under κ-th fold of cross-validation for Abalone dataset in terms of classical/quantum basic probability level decision-making.

Method	Shots	κ-th fold of cross-validation					Acc
		1	2	3	4	5	
DRC	–	1.0000	1.0000	0.9767	1.0000	0.9348	0.9823
QC-DRC$_{\mathrm{QBP}}$	32	0.9535	1.0000	0.9535	0.9767	0.8261	0.9420
	64	0.9535	0.9767	0.9302	1.0000	0.8913	0.9504
	128	1.0000	1.0000	0.9535	0.9767	0.8696	0.9600
	256	1.0000	0.9767	0.9535	1.0000	0.9130	0.9687
	512	1.0000	1.0000	0.9767	1.0000	0.9348	0.9823
	1024	1.0000	1.0000	0.9767	1.0000	0.9565	0.9867
	2048	1.0000	1.0000	0.9767	1.0000	0.9348	0.9823
	4096	1.0000	1.0000	1.0000	1.0000	0.9348	0.9870
	8192	1.0000	1.0000	0.9767	1.0000	0.9348	0.9823
	16384	1.0000	1.0000	0.9767	1.0000	0.9348	0.9823
AQC-DRC$_{\mathrm{QBP}}$	32	1.0000	1.0000	0.9767	1.0000	0.9565	0.9867
	64	1.0000	0.9767	0.9767	1.0000	0.9348	0.9777
	128	1.0000	1.0000	0.9767	1.0000	0.9348	0.9823
	256	1.0000	1.0000	0.9767	1.0000	0.9565	0.9867
	512	1.0000	1.0000	0.9767	1.0000	0.9348	0.9823
	1024	1.0000	1.0000	0.9767	1.0000	0.9348	0.9823
	2048	1.0000	1.0000	0.9767	1.0000	0.9348	0.9823
	4096	1.0000	1.0000	0.9767	1.0000	0.9348	0.9823
	8192	1.0000	1.0000	0.9767	1.0000	0.9348	0.9823
	16384	1.0000	1.0000	0.9767	1.0000	0.9348	0.9823

Table A4: Comparison of classification accuracies under κ-th fold of cross-validation for Abalone dataset in terms of classical/quantum plausibility level decision-making.

Method	Shots	κ-th fold of cross-validation					Acc
		1	2	3	4	5	
DRC+QPl	–	1.0000	1.0000	0.9767	1.0000	0.9348	0.9823
QC-DRC$_{\mathrm{QBP}}$+QPl	32	1.0000	0.9767	1.0000	1.0000	0.9348	0.9823
	64	1.0000	1.0000	1.0000	1.0000	0.9348	0.9870
	128	1.0000	1.0000	0.9767	1.0000	0.9348	0.9823
	256	1.0000	1.0000	0.9767	1.0000	0.9565	0.9867
	512	1.0000	1.0000	0.9767	1.0000	0.9565	0.9867
	1024	1.0000	1.0000	0.9767	1.0000	0.9348	0.9823
	2048	1.0000	1.0000	0.9767	1.0000	0.9348	0.9823
	4096	1.0000	1.0000	0.9767	1.0000	0.9348	0.9823
	8192	1.0000	1.0000	0.9767	1.0000	0.9348	0.9823
	16384	1.0000	1.0000	0.9767	1.0000	0.9348	0.9823
AQC-DRC$_{\mathrm{QBP}}$+QPl	32	0.9070	1.0000	0.9535	0.9070	0.7609	0.9057
	64	0.9535	0.9767	0.9535	1.0000	0.8478	0.9463
	128	1.0000	0.9767	0.9535	0.9767	0.8913	0.9597
	256	1.0000	1.0000	0.9767	1.0000	0.9348	0.9823
	512	1.0000	0.9767	0.9767	1.0000	0.9348	0.9777
	1024	1.0000	1.0000	1.0000	1.0000	0.9565	0.9913
	2048	1.0000	1.0000	0.9767	1.0000	0.9348	0.9823
	4096	1.0000	1.0000	0.9767	1.0000	0.9348	0.9823
	8192	1.0000	1.0000	0.9767	1.0000	0.9565	0.9867
	16384	1.0000	1.0000	0.9767	1.0000	0.9348	0.9823
AQC-DRC$_{\mathrm{QPl}}$	32	0.9767	0.9767	0.9302	0.9070	0.8261	0.9234
	64	1.0000	0.9767	0.9767	1.0000	0.8261	0.9559
	128	1.0000	0.9767	0.9767	1.0000	0.9565	0.9820
	256	1.0000	0.9767	0.9767	1.0000	0.9348	0.9777
	512	1.0000	0.9767	0.9767	1.0000	0.9348	0.9777
	1024	1.0000	0.9767	1.0000	1.0000	0.9348	0.9823
	2048	1.0000	0.9767	0.9767	1.0000	0.9348	0.9777
	4096	1.0000	1.0000	0.9767	1.0000	0.9348	0.9823
	8192	1.0000	1.0000	0.9767	1.0000	0.9348	0.9823
	16384	1.0000	1.0000	0.9767	1.0000	0.9348	0.9823

Table A5: Comparison of classification accuracies under κ-th fold of cross-validation for Knowledge dataset in terms of classical/quantum basic probability level decision-making.

Method	Shots	κ-th fold of cross-validation					Acc
		1	2	3	4	5	
DRC	–	0.8667	0.8312	0.8267	0.8592	0.8861	0.8539
QC-DRC$_{\text{QBP}}$	32	0.6267	0.5455	0.6133	0.5775	0.6582	0.6042
	64	0.8000	0.6883	0.6667	0.7324	0.6456	0.7066
	128	0.7467	0.8052	0.6800	0.7887	0.7595	0.7560
	256	0.8533	0.7792	0.7733	0.8028	0.8481	0.8114
	512	0.8667	0.7922	0.8400	0.8169	0.8354	0.8302
	1024	0.8667	0.7922	0.8667	0.8451	0.8734	0.8488
	2048	0.8667	0.8052	0.8400	0.8451	0.8861	0.8486
	4096	0.8667	0.8312	0.8000	0.8592	0.8987	0.8511
	8192	0.8800	0.8182	0.8400	0.8873	0.8861	0.8623
	16384	0.8667	0.8442	0.8267	0.8310	0.8861	0.8509
AQC-DRC$_{\text{QBP}}$	32	0.6400	0.5844	0.6800	0.5634	0.6329	0.6201
	64	0.6800	0.6883	0.6000	0.7183	0.6962	0.6766
	128	0.6933	0.7532	0.7333	0.7183	0.7468	0.7290
	256	0.7467	0.7532	0.7600	0.7606	0.8861	0.7813
	512	0.8667	0.8052	0.8133	0.8169	0.8101	0.8224
	1024	0.8667	0.7532	0.7733	0.8592	0.8987	0.8302
	2048	0.8800	0.8182	0.8400	0.8169	0.8734	0.8457
	4096	0.8800	0.8182	0.8267	0.8592	0.8734	0.8515
	8192	0.8667	0.8052	0.8267	0.8592	0.8734	0.8462
	16384	0.8800	0.8312	0.8267	0.8451	0.8861	0.8538

Table A6: Comparison of classification accuracies under κ-th fold of cross-validation for Knowledge dataset in terms of classical/quantum plausibility level decision-making.

Method	Shots	κ-th fold of cross-validation					Acc
		1	2	3	4	5	
DRC+QPl	–	0.8667	0.8571	0.8267	0.8592	0.8861	0.8591
QC-DRC$_{\text{QBP}}$+QPl	32	0.6267	0.5844	0.6267	0.6479	0.7089	0.6389
	64	0.7333	0.7013	0.6133	0.6901	0.7342	0.6945
	128	0.7600	0.7403	0.7067	0.7887	0.7215	0.7434
	256	0.7467	0.7403	0.7867	0.8028	0.8481	0.7849
	512	0.8267	0.8442	0.8133	0.8592	0.8354	0.8358
	1024	0.8533	0.8442	0.8400	0.8451	0.8481	0.8461
	2048	0.8667	0.8182	0.8400	0.8451	0.8734	0.8487
	4096	0.8667	0.8442	0.8533	0.8732	0.8861	0.8647
	8192	0.8533	0.8312	0.8533	0.8732	0.8861	0.8594
	16384	0.8667	0.8571	0.8267	0.8592	0.8861	0.8591
AQC-DRC$_{\text{QBP}}$+QPl	32	0.6000	0.6494	0.5600	0.5915	0.6203	0.6042
	64	0.7200	0.7403	0.6533	0.7183	0.7468	0.7157
	128	0.7467	0.7792	0.7333	0.8310	0.8354	0.7851
	256	0.8133	0.7532	0.7733	0.7746	0.8481	0.7925
	512	0.8267	0.8182	0.8400	0.8169	0.8734	0.8350
	1024	0.8667	0.8442	0.8400	0.8873	0.8861	0.8648
	2048	0.8400	0.8571	0.8400	0.8592	0.8861	0.8565
	4096	0.8533	0.8442	0.8267	0.8451	0.8861	0.8511
	8192	0.8667	0.8442	0.8400	0.8732	0.8861	0.8620
	16384	0.8667	0.8571	0.8267	0.8732	0.8861	0.8620
AQC-DRC$_{\text{QPl}}$	32	0.6133	0.6753	0.6533	0.7042	0.6203	0.6533
	64	0.7067	0.7403	0.6933	0.7324	0.7595	0.7264
	128	0.8133	0.7403	0.8000	0.7324	0.7722	0.7716
	256	0.8133	0.7662	0.8133	0.8169	0.8734	0.8166
	512	0.8667	0.7662	0.8000	0.8310	0.8608	0.8249
	1024	0.8533	0.8182	0.8267	0.8732	0.8861	0.8515
	2048	0.8533	0.8312	0.8133	0.8732	0.8987	0.8540
	4096	0.8533	0.8442	0.8267	0.8592	0.8734	0.8513
	8192	0.8667	0.8312	0.8133	0.8592	0.8861	0.8513
	16384	0.8667	0.8571	0.8133	0.8592	0.8861	0.8565

Table A7: Comparison of Dif and StD metrics under κ-fold cross-validation for Iris dataset in terms of quantum basic probability level decision-making.

Method	Shots	κ-th fold of cross-validation					Dif	StD
		1	2	3	4	5		
QC-DRC$_{\text{QBP}}$	32	0.1000	0.1000	0.1000	0.0667	0.1333	0.1000	0.0211
	64	0.0667	0.1000	0.0333	0.0333	0.1000	0.0667	0.0298
	128	0.0000	0.1000	0.0667	0.0333	0.0667	0.0533	0.0340
	256	0.0000	0.0000	0.0333	0.0667	0.0333	0.0267	0.0249
	512	0.0000	0.0333	0.0333	0.0000	0.0333	0.0200	0.0163
	1024	0.0000	0.0667	0.0000	0.0333	0.0333	0.0267	0.0249
	2048	0.0000	0.0333	0.0333	0.0000	0.0000	0.0133	0.0163
	4096	0.0000	0.0333	0.0000	0.0333	0.0000	0.0133	0.0163
	8192	0.0000	0.0000	0.0000	0.0000	0.0333	0.0067	0.0133
	16384	0.0000	0.0000	0.0000	0.0000	0.0000	0.0000	0.0000
AQC-DRC$_{\text{QBP}}$	32	0.1000	0.1667	0.0000	0.0667	0.0667	0.0800	0.0542
	64	0.1000	0.1000	0.0333	0.0667	0.0667	0.0733	0.0249
	128	0.0333	0.0667	0.0333	0.0333	0.1000	0.0533	0.0267
	256	0.0000	0.0000	0.0667	0.0000	0.0000	0.0133	0.0267
	512	0.0000	0.0000	0.0000	0.0333	0.0000	0.0067	0.0133
	1024	0.0000	0.0667	0.0333	0.0333	0.0000	0.0267	0.0249
	2048	0.0000	0.0333	0.0333	0.0000	0.0333	0.0200	0.0163
	4096	0.0000	0.0333	0.0667	0.0000	0.0333	0.0267	0.0249
	8192	0.0000	0.0333	0.0000	0.0000	0.0333	0.0133	0.0163
	16384	0.0000	0.0333	0.0333	0.0000	0.0333	0.0200	0.0163

Table A8: Comparison of Dif and StD metrics under κ-fold cross-validation for Iris dataset in terms of quantum plausibility level decision-making.

Method	Shots	κ-th fold of cross-validation					Dif	StD
		1	2	3	4	5		
QC-DRC$_{\text{QBP}}$+QPl	32	0.1000	0.1667	0.1000	0.1667	0.1333	0.1333	0.0298
	64	0.1333	0.1667	0.0667	0.1000	0.1000	0.1133	0.0340
	128	0.0000	0.0333	0.0333	0.0000	0.1000	0.0333	0.0365
	256	0.0000	0.0333	0.0667	0.0000	0.0667	0.0333	0.0298
	512	0.0000	0.0333	0.0333	0.0333	0.0333	0.0267	0.0133
	1024	0.0000	0.0000	0.0667	0.0333	0.0333	0.0267	0.0249
	2048	0.0000	0.0333	0.0000	0.0333	0.0333	0.0200	0.0163
	4096	0.0000	0.0333	0.0000	0.0000	0.0000	0.0067	0.0133
	8192	0.0000	0.0000	0.0333	0.0000	0.0333	0.0133	0.0163
	16384	0.0000	0.0000	0.0000	0.0000	0.0000	0.0000	0.0000
AQC-DRC$_{\text{QBP}}$+QPl	32	0.0333	0.0667	0.0667	0.0667	0.1000	0.0667	0.0211
	64	0.1000	0.0667	0.0667	0.0333	0.0000	0.0533	0.0340
	128	0.0000	0.0667	0.0333	0.0667	0.0333	0.0400	0.0249
	256	0.0000	0.0667	0.0333	0.0000	0.0000	0.0200	0.0267
	512	0.0000	0.0667	0.0667	0.0000	0.0000	0.0267	0.0327
	1024	0.0000	0.0333	0.0667	0.0000	0.0000	0.0200	0.0267
	2048	0.0000	0.0000	0.0000	0.0000	0.0000	0.0000	0.0000
	4096	0.0000	0.0333	0.0333	0.0000	0.0333	0.0200	0.0163
	8192	0.0000	0.0333	0.0333	0.0000	0.0000	0.0133	0.0163
	16384	0.0000	0.0000	0.0333	0.0000	0.0000	0.0067	0.0133
AQC-DRC$_{\text{QPl}}$	32	0.0333	0.1000	0.0333	0.0667	0.0333	0.0533	0.0267
	64	0.0000	0.1333	0.0667	0.0000	0.1000	0.0600	0.0533
	128	0.0000	0.1000	0.0667	0.0000	0.0000	0.0333	0.0422
	256	0.0000	0.0333	0.0000	0.0333	0.0000	0.0133	0.0163
	512	0.0000	0.0333	0.0000	0.0333	0.0000	0.0133	0.0163
	1024	0.0000	0.0333	0.0000	0.0000	0.0000	0.0067	0.0133
	2048	0.0000	0.0000	0.0333	0.0000	0.0000	0.0067	0.0133
	4096	0.0000	0.0333	0.0000	0.0000	0.0333	0.0133	0.0163
	8192	0.0000	0.0333	0.0333	0.0000	0.0000	0.0133	0.0163
	16384	0.0000	0.0333	0.0000	0.0000	0.0000	0.0067	0.0133

Table A9: Comparison of Dif and StD metrics under κ-fold cross-validation for Abalone dataset in terms of quantum basic probability level decision-making.

Method	Shots	κ-th fold of cross-validation					Dif	StD
		1	2	3	4	5		
QC-DRC$_{\text{QBP}}$	32	0.0465	0.0000	0.0233	0.0233	0.1522	0.0490	0.0536
	64	0.0465	0.0233	0.0465	0.0000	0.0870	0.0406	0.0289
	128	0.0000	0.0000	0.0233	0.0233	0.0652	0.0223	0.0238
	256	0.0000	0.0233	0.0233	0.0000	0.0217	0.0137	0.0112
	512	0.0000	0.0000	0.0000	0.0000	0.0000	0.0000	0.0000
	1024	0.0000	0.0000	0.0000	0.0000	0.0217	0.0043	0.0087
	2048	0.0000	0.0000	0.0000	0.0000	0.0000	0.0000	0.0000
	4096	0.0000	0.0000	0.0233	0.0000	0.0000	0.0047	0.0093
	8192	0.0000	0.0000	0.0000	0.0000	0.0000	0.0000	0.0000
	16384	0.0000	0.0000	0.0000	0.0000	0.0000	0.0000	0.0000
AQC-DRC$_{\text{QBP}}$	32	0.0000	0.0000	0.0000	0.0000	0.0217	0.0043	0.0087
	64	0.0000	0.0233	0.0000	0.0000	0.0000	0.0047	0.0093
	128	0.0000	0.0000	0.0000	0.0000	0.0000	0.0000	0.0000
	256	0.0000	0.0000	0.0000	0.0000	0.0217	0.0043	0.0087
	512	0.0000	0.0000	0.0000	0.0000	0.0000	0.0000	0.0000
	1024	0.0000	0.0000	0.0000	0.0000	0.0000	0.0000	0.0000
	2048	0.0000	0.0000	0.0000	0.0000	0.0000	0.0000	0.0000
	4096	0.0000	0.0000	0.0000	0.0000	0.0000	0.0000	0.0000
	8192	0.0000	0.0000	0.0000	0.0000	0.0000	0.0000	0.0000
	16384	0.0000	0.0000	0.0000	0.0000	0.0000	0.0000	0.0000

Table A10: Comparison of Dif and StD metrics under κ-fold cross-validation for Abalone dataset in terms of quantum plausibility level decision-making.

Method	Shots	κ-th fold of cross-validation					Dif	StD
		1	2	3	4	5		
QC-DRC$_{\text{QBP}}$+QPl	32	0.0000	0.0233	0.0233	0.0000	0.0000	0.0093	0.0114
	64	0.0000	0.0000	0.0233	0.0000	0.0000	0.0047	0.0093
	128	0.0000	0.0000	0.0000	0.0000	0.0000	0.0000	0.0000
	256	0.0000	0.0000	0.0000	0.0000	0.0217	0.0043	0.0087
	512	0.0000	0.0000	0.0000	0.0000	0.0217	0.0043	0.0087
	1024	0.0000	0.0000	0.0000	0.0000	0.0000	0.0000	0.0000
	2048	0.0000	0.0000	0.0000	0.0000	0.0000	0.0000	0.0000
	4096	0.0000	0.0000	0.0000	0.0000	0.0000	0.0000	0.0000
	8192	0.0000	0.0000	0.0000	0.0000	0.0000	0.0000	0.0000
	16384	0.0000	0.0000	0.0000	0.0000	0.0000	0.0000	0.0000
AQC-DRC$_{\text{QBP}}$+QPl	32	0.0930	0.0000	0.0233	0.0930	0.1739	0.0766	0.0612
	64	0.0465	0.0233	0.0233	0.0000	0.1304	0.0447	0.0453
	128	0.0000	0.0233	0.0233	0.0233	0.0435	0.0226	0.0138
	256	0.0000	0.0000	0.0000	0.0000	0.0000	0.0000	0.0000
	512	0.0000	0.0233	0.0000	0.0000	0.0000	0.0047	0.0093
	1024	0.0000	0.0000	0.0233	0.0000	0.0217	0.0090	0.0110
	2048	0.0000	0.0000	0.0000	0.0000	0.0000	0.0000	0.0000
	4096	0.0000	0.0000	0.0000	0.0000	0.0000	0.0000	0.0000
	8192	0.0000	0.0000	0.0000	0.0000	0.0217	0.0043	0.0087
	16384	0.0000	0.0000	0.0000	0.0000	0.0000	0.0000	0.0000
AQC-DRC$_{\text{QPl}}$	32	0.0233	0.0233	0.0465	0.0930	0.1522	0.0676	0.0493
	64	0.0000	0.0233	0.0465	0.0000	0.1087	0.0357	0.0404
	128	0.0000	0.0233	0.0000	0.0000	0.0217	0.0090	0.0110
	256	0.0000	0.0233	0.0465	0.0000	0.0000	0.0140	0.0186
	512	0.0000	0.0233	0.0000	0.0000	0.0000	0.0047	0.0093
	1024	0.0000	0.0233	0.0233	0.0000	0.0000	0.0093	0.0114
	2048	0.0000	0.0233	0.0000	0.0000	0.0000	0.0047	0.0093
	4096	0.0000	0.0000	0.0000	0.0000	0.0000	0.0000	0.0000
	8192	0.0000	0.0000	0.0000	0.0000	0.0000	0.0000	0.0000
	16384	0.0000	0.0000	0.0000	0.0000	0.0000	0.0000	0.0000

Table A11: Comparison of Dif and StD metrics under κ-fold cross-validation for Knowledge dataset in terms of quantum basic probability level decision-making.

Method	Shots	κ-th fold of cross-validation					Dif	StD
		1	2	3	4	5		
QC-DRC$_{\text{QBP}}$	32	0.3200	0.3117	0.2933	0.3380	0.2785	0.3083	0.0207
	64	0.1200	0.2727	0.2133	0.1831	0.2911	0.2161	0.0619
	128	0.1467	0.1039	0.2267	0.1549	0.1772	0.1619	0.0402
	256	0.0400	0.0779	0.1067	0.1408	0.0633	0.0857	0.0350
	512	0.0000	0.0649	0.0400	0.0704	0.0506	0.0452	0.0250
	1024	0.0000	0.0649	0.0667	0.0423	0.0380	0.0424	0.0241
	2048	0.0000	0.0779	0.0667	0.0141	0.0000	0.0317	0.0337
	4096	0.0000	0.0519	0.0267	0.0563	0.0127	0.0295	0.0218
	8192	0.0133	0.0130	0.0400	0.0563	0.0000	0.0245	0.0205
	16384	0.0000	0.0130	0.0000	0.0563	0.0000	0.0139	0.0218
AQC-DRC$_{\text{QBP}}$	32	0.3333	0.3766	0.2800	0.3803	0.3038	0.3348	0.0395
	64	0.2667	0.2208	0.3067	0.1690	0.2658	0.2458	0.0470
	128	0.1733	0.1818	0.1467	0.1690	0.1646	0.1671	0.0117
	256	0.1200	0.2078	0.1200	0.1268	0.0253	0.1200	0.0578
	512	0.0267	0.0779	0.0400	0.1268	0.0759	0.0695	0.0349
	1024	0.0267	0.0779	0.1067	0.0563	0.0380	0.0611	0.0286
	2048	0.0133	0.0130	0.0133	0.0423	0.0127	0.0189	0.0117
	4096	0.0133	0.0390	0.0267	0.0282	0.0127	0.0240	0.0099
	8192	0.0000	0.0779	0.0267	0.0000	0.0127	0.0234	0.0290
	16384	0.0133	0.0260	0.0000	0.0141	0.0000	0.0107	0.0098

Table A12: Comparison of Dif and StD metrics under κ-fold cross-validation for Knowledge dataset in terms of quantum plausibility level decision-making.

Method	Shots	κ-th fold of cross-validation					Dif	StD
		1	2	3	4	5		
QC-DRC$_{\text{QBP}}$+QPl	32	0.2933	0.3247	0.3600	0.2958	0.3038	0.3155	0.0248
	64	0.2133	0.2078	0.2933	0.2254	0.2025	0.2285	0.0333
	128	0.1333	0.1429	0.1733	0.1268	0.1899	0.1532	0.0243
	256	0.1200	0.1688	0.1200	0.1408	0.0886	0.1277	0.0265
	512	0.0400	0.0649	0.0933	0.0845	0.0759	0.0717	0.0184
	1024	0.0133	0.0390	0.0933	0.0423	0.0380	0.0452	0.0262
	2048	0.0267	0.0390	0.0400	0.0423	0.0127	0.0321	0.0111
	4096	0.0000	0.0130	0.0267	0.0141	0.0000	0.0107	0.0100
	8192	0.0133	0.0260	0.0533	0.0141	0.0000	0.0213	0.0180
	16384	0.0000	0.0000	0.0533	0.0282	0.0000	0.0163	0.0215
AQC-DRC$_{\text{QBP}}$+QPl	32	0.2667	0.2857	0.3467	0.2958	0.3165	0.3023	0.0274
	64	0.1733	0.1688	0.2800	0.1972	0.1899	0.2018	0.0404
	128	0.1200	0.1299	0.1467	0.0563	0.1266	0.1159	0.0310
	256	0.0533	0.1558	0.1067	0.0845	0.0886	0.0978	0.0337
	512	0.0400	0.1169	0.0400	0.0986	0.0127	0.0616	0.0394
	1024	0.0000	0.0130	0.0400	0.0282	0.0253	0.0213	0.0137
	2048	0.0267	0.0000	0.0400	0.0563	0.0253	0.0297	0.0186
	4096	0.0133	0.0130	0.0800	0.0423	0.0000	0.0297	0.0287
	8192	0.0000	0.0390	0.0400	0.0141	0.0000	0.0186	0.0178
	16384	0.0000	0.0000	0.0533	0.0141	0.0000	0.0135	0.0207
AQC-DRC$_{\text{QPl}}$	32	0.3067	0.3117	0.3867	0.2113	0.3418	0.3116	0.0577
	64	0.1600	0.1948	0.1867	0.2113	0.2278	0.1961	0.0229
	128	0.0800	0.1429	0.0800	0.1831	0.1139	0.1200	0.0393
	256	0.0533	0.0909	0.0400	0.0704	0.0380	0.0585	0.0199
	512	0.0533	0.1169	0.0533	0.0563	0.0506	0.0661	0.0255
	1024	0.0400	0.0390	0.0800	0.0141	0.0000	0.0346	0.0273
	2048	0.0133	0.0260	0.0667	0.0141	0.0127	0.0265	0.0207
	4096	0.0133	0.0130	0.0000	0.0282	0.0380	0.0185	0.0132
	8192	0.0000	0.0260	0.0133	0.0000	0.0000	0.0079	0.0104
	16384	0.0000	0.0000	0.0400	0.0282	0.0000	0.0136	0.0171

NeurIPS Paper Checklist

1. **Claims**

   Question: Do the main claims made in the abstract and introduction accurately reflect the paper's contributions and scope?

   Answer: [Yes]

   Justification: The main claims made in the abstract and introduction accurately reflect the paper's contributions and scope.

   Guidelines:

   - The answer NA means that the abstract and introduction do not include the claims made in the paper.
   - The abstract and/or introduction should clearly state the claims made, including the contributions made in the paper and important assumptions and limitations. A No or NA answer to this question will not be perceived well by the reviewers.
   - The claims made should match theoretical and experimental results, and reflect how much the results can be expected to generalize to other settings.
   - It is fine to include aspirational goals as motivation as long as it is clear that these goals are not attained by the paper.

2. **Limitations**

   Question: Does the paper discuss the limitations of the work performed by the authors?

   Answer: [Yes]

   Justification: The limitations of the work were discussed in Section 6.

   Guidelines:

   - The answer NA means that the paper has no limitation while the answer No means that the paper has limitations, but those are not discussed in the paper.
   - The authors are encouraged to create a separate "Limitations" section in their paper.
   - The paper should point out any strong assumptions and how robust the results are to violations of these assumptions (e.g., independence assumptions, noiseless settings, model well-specification, asymptotic approximations only holding locally). The authors should reflect on how these assumptions might be violated in practice and what the implications would be.
   - The authors should reflect on the scope of the claims made, e.g., if the approach was only tested on a few datasets or with a few runs. In general, empirical results often depend on implicit assumptions, which should be articulated.
   - The authors should reflect on the factors that influence the performance of the approach. For example, a facial recognition algorithm may perform poorly when image resolution is low or images are taken in low lighting. Or a speech-to-text system might not be used reliably to provide closed captions for online lectures because it fails to handle technical jargon.
   - The authors should discuss the computational efficiency of the proposed algorithms and how they scale with dataset size.
   - If applicable, the authors should discuss possible limitations of their approach to address problems of privacy and fairness.
   - While the authors might fear that complete honesty about limitations might be used by reviewers as grounds for rejection, a worse outcome might be that reviewers discover limitations that aren't acknowledged in the paper. The authors should use their best judgment and recognize that individual actions in favor of transparency play an important role in developing norms that preserve the integrity of the community. Reviewers will be specifically instructed to not penalize honesty concerning limitations.

3. **Theory assumptions and proofs**

   Question: For each theoretical result, does the paper provide the full set of assumptions and a complete (and correct) proof?

   Answer: [Yes]

Justification: All of the assumptions and proofs of proposed AQC-DRC can be found in Section 3.

Guidelines:

- The answer NA means that the paper does not include theoretical results.
- All the theorems, formulas, and proofs in the paper should be numbered and cross-referenced.
- All assumptions should be clearly stated or referenced in the statement of any theorems.
- The proofs can either appear in the main paper or the supplemental material, but if they appear in the supplemental material, the authors are encouraged to provide a short proof sketch to provide intuition.
- Inversely, any informal proof provided in the core of the paper should be complemented by formal proofs provided in appendix or supplemental material.
- Theorems and Lemmas that the proof relies upon should be properly referenced.

4. **Experimental result reproducibility**

   Question: Does the paper fully disclose all the information needed to reproduce the main experimental results of the paper to the extent that it affects the main claims and/or conclusions of the paper (regardless of whether the code and data are provided or not)?

   Answer: [Yes]

   Justification: All the information needed to reproduce the main experimental results of the paper is shown in Section 4

   Guidelines:

   - The answer NA means that the paper does not include experiments.
   - If the paper includes experiments, a No answer to this question will not be perceived well by the reviewers: Making the paper reproducible is important, regardless of whether the code and data are provided or not.
   - If the contribution is a dataset and/or model, the authors should describe the steps taken to make their results reproducible or verifiable.
   - Depending on the contribution, reproducibility can be accomplished in various ways. For example, if the contribution is a novel architecture, describing the architecture fully might suffice, or if the contribution is a specific model and empirical evaluation, it may be necessary to either make it possible for others to replicate the model with the same dataset, or provide access to the model. In general. releasing code and data is often one good way to accomplish this, but reproducibility can also be provided via detailed instructions for how to replicate the results, access to a hosted model (e.g., in the case of a large language model), releasing of a model checkpoint, or other means that are appropriate to the research performed.
   - While NeurIPS does not require releasing code, the conference does require all submissions to provide some reasonable avenue for reproducibility, which may depend on the nature of the contribution. For example
     (a) If the contribution is primarily a new algorithm, the paper should make it clear how to reproduce that algorithm.
     (b) If the contribution is primarily a new model architecture, the paper should describe the architecture clearly and fully.
     (c) If the contribution is a new model (e.g., a large language model), then there should either be a way to access this model for reproducing the results or a way to reproduce the model (e.g., with an open-source dataset or instructions for how to construct the dataset).
     (d) We recognize that reproducibility may be tricky in some cases, in which case authors are welcome to describe the particular way they provide for reproducibility. In the case of closed-source models, it may be that access to the model is limited in some way (e.g., to registered users), but it should be possible for other researchers to have some path to reproducing or verifying the results.

5. **Open access to data and code**

Question: Does the paper provide open access to the data and code, with sufficient instructions to faithfully reproduce the main experimental results, as described in supplemental material?

Answer: [No]

Justification: Sufficient instructions to faithfully reproduce the main experimental results were provided in Sections 3 and 4, with the datasets described in Section 4. To protect the intellectual property during the review process, we do not release the code publicly at this stage. The code will be available upon request after publication.

Guidelines:

- The answer NA means that paper does not include experiments requiring code.
- Please see the NeurIPS code and data submission guidelines (`https://nips.cc/public/guides/CodeSubmissionPolicy`) for more details.
- While we encourage the release of code and data, we understand that this might not be possible, so No is an acceptable answer. Papers cannot be rejected simply for not including code, unless this is central to the contribution (e.g., for a new open-source benchmark).
- The instructions should contain the exact command and environment needed to run to reproduce the results. See the NeurIPS code and data submission guidelines (`https://nips.cc/public/guides/CodeSubmissionPolicy`) for more details.
- The authors should provide instructions on data access and preparation, including how to access the raw data, preprocessed data, intermediate data, and generated data, etc.
- The authors should provide scripts to reproduce all experimental results for the new proposed method and baselines. If only a subset of experiments are reproducible, they should state which ones are omitted from the script and why.
- At submission time, to preserve anonymity, the authors should release anonymized versions (if applicable).
- Providing as much information as possible in supplemental material (appended to the paper) is recommended, but including URLs to data and code is permitted.

6. **Experimental setting/details**

Question: Does the paper specify all the training and test details (e.g., data splits, hyperparameters, how they were chosen, type of optimizer, etc.) necessary to understand the results?

Answer: [Yes]

Justification: The detailed data-splitting process was shown in Section 4. The hyperparameter in our algorithm 'shots' was also analyzed in Section 4. There was no optimizer needed in our algorithm.

Guidelines:

- The answer NA means that the paper does not include experiments.
- The experimental setting should be presented in the core of the paper to a level of detail that is necessary to appreciate the results and make sense of them.
- The full details can be provided either with the code, in appendix, or as supplemental material.

7. **Experiment statistical significance**

Question: Does the paper report error bars suitably and correctly defined or other appropriate information about the statistical significance of the experiments?

Answer: [Yes]

Justification: The experimental results Dif in Figure 2 reported error bars suitably and correctly defined in Section 4.

Guidelines:

- The answer NA means that the paper does not include experiments.
- The authors should answer "Yes" if the results are accompanied by error bars, confidence intervals, or statistical significance tests, at least for the experiments that support the main claims of the paper.

- The factors of variability that the error bars are capturing should be clearly stated (for example, train/test split, initialization, random drawing of some parameter, or overall run with given experimental conditions).
- The method for calculating the error bars should be explained (closed form formula, call to a library function, bootstrap, etc.)
- The assumptions made should be given (e.g., Normally distributed errors).
- It should be clear whether the error bar is the standard deviation or the standard error of the mean.
- It is OK to report 1-sigma error bars, but one should state it. The authors should preferably report a 2-sigma error bar than state that they have a 96% CI, if the hypothesis of Normality of errors is not verified.
- For asymmetric distributions, the authors should be careful not to show in tables or figures symmetric error bars that would yield results that are out of range (e.g. negative error rates).
- If error bars are reported in tables or plots, The authors should explain in the text how they were calculated and reference the corresponding figures or tables in the text.

8. **Experiments compute resources**

   Question: For each experiment, does the paper provide sufficient information on the computer resources (type of compute workers, memory, time of execution) needed to reproduce the experiments?

   Answer: [Yes]

   Justification: The experiments environment is provided in Appendix A2.

   Guidelines:

   - The answer NA means that the paper does not include experiments.
   - The paper should indicate the type of compute workers CPU or GPU, internal cluster, or cloud provider, including relevant memory and storage.
   - The paper should provide the amount of compute required for each of the individual experimental runs as well as estimate the total compute.
   - The paper should disclose whether the full research project required more compute than the experiments reported in the paper (e.g., preliminary or failed experiments that didn't make it into the paper).

9. **Code of ethics**

   Question: Does the research conducted in the paper conform, in every respect, with the NeurIPS Code of Ethics `https://neurips.cc/public/EthicsGuidelines`?

   Answer: [Yes]

   Justification: We have read the NeurIPS Code of Ethics and do not find our work in violation of any aspects.

   Guidelines:

   - The answer NA means that the authors have not reviewed the NeurIPS Code of Ethics.
   - If the authors answer No, they should explain the special circumstances that require a deviation from the Code of Ethics.
   - The authors should make sure to preserve anonymity (e.g., if there is a special consideration due to laws or regulations in their jurisdiction).

10. **Broader impacts**

    Question: Does the paper discuss both potential positive societal impacts and negative societal impacts of the work performed?

    Answer: [NA]

    Justification: Our work is a quantum algorithm for uncertain pattern classification that does not involve ethics and therefore has no impact on society.

    Guidelines:

    - The answer NA means that there is no societal impact of the work performed.

- If the authors answer NA or No, they should explain why their work has no societal impact or why the paper does not address societal impact.
- Examples of negative societal impacts include potential malicious or unintended uses (e.g., disinformation, generating fake profiles, surveillance), fairness considerations (e.g., deployment of technologies that could make decisions that unfairly impact specific groups), privacy considerations, and security considerations.
- The conference expects that many papers will be foundational research and not tied to particular applications, let alone deployments. However, if there is a direct path to any negative applications, the authors should point it out. For example, it is legitimate to point out that an improvement in the quality of generative models could be used to generate deepfakes for disinformation. On the other hand, it is not needed to point out that a generic algorithm for optimizing neural networks could enable people to train models that generate Deepfakes faster.
- The authors should consider possible harms that could arise when the technology is being used as intended and functioning correctly, harms that could arise when the technology is being used as intended but gives incorrect results, and harms following from (intentional or unintentional) misuse of the technology.
- If there are negative societal impacts, the authors could also discuss possible mitigation strategies (e.g., gated release of models, providing defenses in addition to attacks, mechanisms for monitoring misuse, mechanisms to monitor how a system learns from feedback over time, improving the efficiency and accessibility of ML).

11. **Safeguards**

    Question: Does the paper describe safeguards that have been put in place for responsible release of data or models that have a high risk for misuse (e.g., pretrained language models, image generators, or scraped datasets)?

    Answer: [NA]

    Justification: Our work does not create any dataset or pretrained model.

    Guidelines:

    - The answer NA means that the paper poses no such risks.
    - Released models that have a high risk for misuse or dual-use should be released with necessary safeguards to allow for controlled use of the model, for example by requiring that users adhere to usage guidelines or restrictions to access the model or implementing safety filters.
    - Datasets that have been scraped from the Internet could pose safety risks. The authors should describe how they avoided releasing unsafe images.
    - We recognize that providing effective safeguards is challenging, and many papers do not require this, but we encourage authors to take this into account and make a best faith effort.

12. **Licenses for existing assets**

    Question: Are the creators or original owners of assets (e.g., code, data, models), used in the paper, properly credited and are the license and terms of use explicitly mentioned and properly respected?

    Answer: [Yes]

    Justification: All datasets used in the experiments of our work were properly credited.

    Guidelines:

    - The answer NA means that the paper does not use existing assets.
    - The authors should cite the original paper that produced the code package or dataset.
    - The authors should state which version of the asset is used and, if possible, include a URL.
    - The name of the license (e.g., CC-BY 4.0) should be included for each asset.
    - For scraped data from a particular source (e.g., website), the copyright and terms of service of that source should be provided.

- If assets are released, the license, copyright information, and terms of use in the package should be provided. For popular datasets, `paperswithcode.com/datasets` has curated licenses for some datasets. Their licensing guide can help determine the license of a dataset.
- For existing datasets that are re-packaged, both the original license and the license of the derived asset (if it has changed) should be provided.
- If this information is not available online, the authors are encouraged to reach out to the asset's creators.

13. **New assets**

    Question: Are new assets introduced in the paper well documented and is the documentation provided alongside the assets?

    Answer: [NA]

    Justification: Our work does not release any new assets.

    Guidelines:

    - The answer NA means that the paper does not release new assets.
    - Researchers should communicate the details of the dataset/code/model as part of their submissions via structured templates. This includes details about training, license, limitations, etc.
    - The paper should discuss whether and how consent was obtained from people whose asset is used.
    - At submission time, remember to anonymize your assets (if applicable). You can either create an anonymized URL or include an anonymized zip file.

14. **Crowdsourcing and research with human subjects**

    Question: For crowdsourcing experiments and research with human subjects, does the paper include the full text of instructions given to participants and screenshots, if applicable, as well as details about compensation (if any)?

    Answer: [NA]

    Justification: Our work does not involve crowdsourcing nor research with human subjects.

    Guidelines:

    - The answer NA means that the paper does not involve crowdsourcing nor research with human subjects.
    - Including this information in the supplemental material is fine, but if the main contribution of the paper involves human subjects, then as much detail as possible should be included in the main paper.
    - According to the NeurIPS Code of Ethics, workers involved in data collection, curation, or other labor should be paid at least the minimum wage in the country of the data collector.

15. **Institutional review board (IRB) approvals or equivalent for research with human subjects**

    Question: Does the paper describe potential risks incurred by study participants, whether such risks were disclosed to the subjects, and whether Institutional Review Board (IRB) approvals (or an equivalent approval/review based on the requirements of your country or institution) were obtained?

    Answer: [NA]

    Justification: Our work does not involve crowdsourcing nor research with human subjects.

    Guidelines:

    - The answer NA means that the paper does not involve crowdsourcing nor research with human subjects.
    - Depending on the country in which research is conducted, IRB approval (or equivalent) may be required for any human subjects research. If you obtained IRB approval, you should clearly state this in the paper.

- We recognize that the procedures for this may vary significantly between institutions and locations, and we expect authors to adhere to the NeurIPS Code of Ethics and the guidelines for their institution.
- For initial submissions, do not include any information that would break anonymity (if applicable), such as the institution conducting the review.

16. **Declaration of LLM usage**

    Question: Does the paper describe the usage of LLMs if it is an important, original, or non-standard component of the core methods in this research? Note that if the LLM is used only for writing, editing, or formatting purposes and does not impact the core methodology, scientific rigorousness, or originality of the research, declaration is not required.

    Answer: [NA]

    Justification: Our work does not involve LLMs as any important, original, or non-standard components.

    Guidelines:

    - The answer NA means that the core method development in this research does not involve LLMs as any important, original, or non-standard components.
    - Please refer to our LLM policy (`https://neurips.cc/Conferences/2025/LLM`) for what should or should not be described.